European Journal of Medicinal Chemistry 304 (2026) 118543

Contents lists available at ScienceDirect

European Journal of Medicinal Chemistry

journal homepage: www.elsevier.com/locate/ejmech

Research paper

Coumarin-stavudine (d4T) novel hybrid ProTides with dual-functionality and enhanced anti-HIV activity

Sahar B. Kandil [a,*], Katie S. Jones [a], Christophe Pannecouque [b], Andrew D. Westwell [a]

[a] School of Pharmacy and Pharmaceutical Sciences, Cardiff University, King Edward VII Avenue, Cardiff, CF10 3NB, UK
[b] Rega Institute for Medical Research - Laboratory of Virology and Chemotherapy, K.U. Leuven, Herestraat 49, Leuven, B-3000, Belgium

ARTICLE INFO

Keywords:
Human immunodeficiency virus (HIV)
Acquired immunodeficiency syndrome (AIDS)
Stavudine (d4T)
Phosphoramidate (ProTide)
Phosphorodiamidate (diamidate)
Coumarin
4-MethylUmbelliferone (4MU)
Hybridisation

ABSTRACT

Innovative anti-HIV strategies are urgently needed to address challenges in vaccine development and multidrug resistance. ProTides are a clinically validated prodrug strategy that improves nucleoside monophosphate delivery by bypassing the first phosphorylation step. Conventional ProTides employ phenol or 1-naphthol aryl groups, which release potentially toxic byproducts upon activation. We report the first use of coumarin-based fluorophores (4MU or 4TFMU) as aryl masking groups in stavudine (d4T) ProTides, creating hybrid profluorophores with dual antiviral and fluorescent tracking capabilities. Eight hybrid ProTides were synthesised and evaluated against HIV-1 (III_B) and HIV-2 (ROD) in MT-4 cells. Five ProTides retained activity in thymidine kinase deficient C8166-TK^- cells, confirming bypass of the first phosphorylation step. ProTide **21** showed potent activity (IC_{50}: 80 nM for HIV-1, 140 nM for HIV-2) and high selectivity indices (1549 and 923), outperforming d4T. Enzymatic activation was verified by ^{31}P NMR. Surprisingly, two phosphorodiamidate derivatives were isolated, revealing a new class of phosphorodiamidating reagents enabling efficient synthesis of diamidate prodrugs. This multifunctional ProTide platform combined enhanced potency, reduced toxicity, and built-in fluorescence, offering promising avenues for next generation nucleoside and non-nucleoside ProTide and diamidate based therapeutics.

1. Introduction

Human Immunodeficiency Virus (HIV) infection causes T-cell deficiency and damages the immune system resulting in chronic acquired immunodeficiency syndrome (AIDS). In 2024, 40.8 million people were living with HIV worldwide and 630,000 deaths were reported, with sub-Saharan Africa disproportionately affected, accounting for 26 million cases and 50 % of new infections [1]. Rising drug resistance, with virologic failure occurring in up to 20 % of individuals receiving first-line antiretroviral therapy (ART) combined with the lack of an approved vaccine, makes HIV a persistent global health challenge, which underscores the need to identify and develop novel anti-HIV compounds [2].

1.1. Nucleoside analogues (NAs)

Nucleosides are the building blocks of nucleic acids (RNA and DNA) and play essential roles in cell signalling and metabolism. Nucleoside analogues (NAs) are structurally modified nucleosides with alterations at the base and/or the sugar moiety [3,4]. NAs are a cornerstone of chemotherapy in cancer and viral infections, including HIV, HBV, HCV, HCMV, HSV, influenza, and SARS-CoV-2 [5]. Over 40 nucleoside and nucleotide analogues are clinically approved and like their natural counterparts, they require three phosphorylation steps, catalysed by intracellular kinases (e.g. thymidine kinase) to generate the active nucleotide triphosphate form (NATP) which subsequently becomes a polymerase or transcriptase substrate. However, structural differences between NAs and natural nucleosides, along with kinase specificity, often result in inefficient phosphorylation, making this process a rate- and activity-limiting step [6]. Over the past 25 years, several strategies have been developed to improve the intracellular delivery of NAs, including the use of monophosphate (NAMP) derivatives. However, these analogues often exhibit increased polarity, limited permeability, and greater susceptibility to enzymatic degradation (e.g. phosphatases). Additional challenges such as rate limiting activation; toxicity concerns; low oral bioavailability; resistance due to downregulation of nucleoside transporters and deamination have further limited the efficacy of this drug class [6]. To address the inefficient kinase-dependent phosphorylation step, the introduction of isoelectric and isosteric phosphonate moiety has improved metabolic stability and cellular uptake compared

* Corresponding author.
E-mail address: Kandils1@cardiff.ac.uk (S.B. Kandil).

https://doi.org/10.1016/j.ejmech.2025.118543
Received 10 October 2025; Received in revised form 24 December 2025; Accepted 28 December 2025
Available online 30 December 2025

to phosphate group as demonstrated by the clinically approved antiviral drugs, such as cidofovir (CMV), adefovir (HBV) and tenofovir (HIV) [5,6].

1.2. Prodrug technology of nucleoside analogues (NAs)

Nucleoside analogues (NAs) typically suffer from poor cellular permeability and slow intracellular generation of the active monophosphate (NAMP) form. To address these limitations, the **Pro**drug nucleo**Tide** (**ProTide**; 5′-aryloxyphosphoramidate) approach, developed by McGuigan in the early 1990s has emerged as the most successful prodrug strategy for antiviral nucleotides with promising applications in antitumour and other chemotherapeutic areas [7–9]. ProTides mask the polar negative charge of NA monophosphates or monophosphonates using a promoiety composed of two protecting groups, thereby enhancing membrane permeability and efficacy. This phosphoramidate promoiety consists of an amino acid ester and an aryl group, typically L-alanine and phenol or 1-naphthol, respectively. Once, inside the cell, ProTides are enzymatically or spontaneously cleaved to release the active monophosphate or phosphonate, which then undergoes further phosphorylation into the active triphosphate form (NATP), thereby inhibiting polymerase or transcriptase enzymes, halting nucleic acid chain elongation and blocking replication, Fig. 1 [9,10].

The application of the ProTide approach to NAs addresses key limitations such as deactivation, dependence on active transport, and inefficient phosphorylation [11]. Currently, three ProTides are FDA approved; sofosbuvir for HCV, tenofovir alafenamide (TAF) as part of combination antiretroviral therapy (cART) for HIV and HBV, and Remdesivir for SARS-CoV-2 [12–14]. Additionally, NUC-3373 is in clinical trials as an anticancer candidate for solid tumours [15]. Numerous other ProTides of antiviral and anticancer NAs have been investigated, such as INX-189 for HCV, Fig. 2 [16,17]. The chemical synthesis of ProTides typically yields a roughly 1:1 mixture of diastereoisomers due to the chirality of the phosphorus atom (R_p/S_p). However, using proline amino acid esters can produce a single phosphorus diastereoisomer, as demonstrated with some proline based BVDU ProTides, owing to the restricted stereochemistry of the cyclic pyrrolidine ring [18]. ProTide diastereoisomers may exhibit distinct biological profiles, although similar activities are sometimes observed [12,18]. Other phosphate and phosphonate NA prodrug strategies include lipid diester and chemical cycloSAL approach [19,20].

In 2011, McGuigan and colleagues developed phosphorodiamidate prodrugs, which use two symmetric or asymmetrical amino acid ester groups to mask the negative charge of the NA monophosphate. Unlike phosphoramidate ProTides, the phosphorus centre in symmetric phosphorodiamidate (diamidate) prodrugs is achiral, eliminating diastereomeric related issues. Moreover, diamidates utilise non-toxic, natural amino acids and avoid the need for non-natural phenol or 1-naphthol aryl groups [21–23].

1.3. Stavudine (d4T) nucleoside

Stavudine (2′,3′-didehydro-2′,3′-dideoxythymidine, d4T), is a clinically approved nucleoside reverse transcriptase inhibitor (NRTI) used in the treatment of HIV infection, Fig. 2. Although, stavudine was once widely used in combination anti-retroviral therapy (cART), the World Health Organisation (WHO) has recommended its phase-out due to toxicity concerns, including severe side effects such as lactic acidosis and hepatic steatosis. Enhancing stavudine's activity through the ProTide approach may allow for lower dosing and reduced toxicity [24]. Stampidine (4-bromophenyl L-alanine methyl ester ProTide of stavudine, d4T) was among the first ProTides to advance into clinical trials, exhibiting potent prophylactic and therapeutic anti-HIV activity, including efficacy against resistant HIV-1 strains. Stampidine is up to 100 times more active than stavudine. Unlike its parent nucleoside stavudine, stampidine demonstrates tolerability and favourable pharmacokinetic profile; but was not approved as a drug. More recently, stampidine has shown chemopreventive efficacy in a murine breast cancer model, highlighting its potential beyond antiviral therapy [25,26].

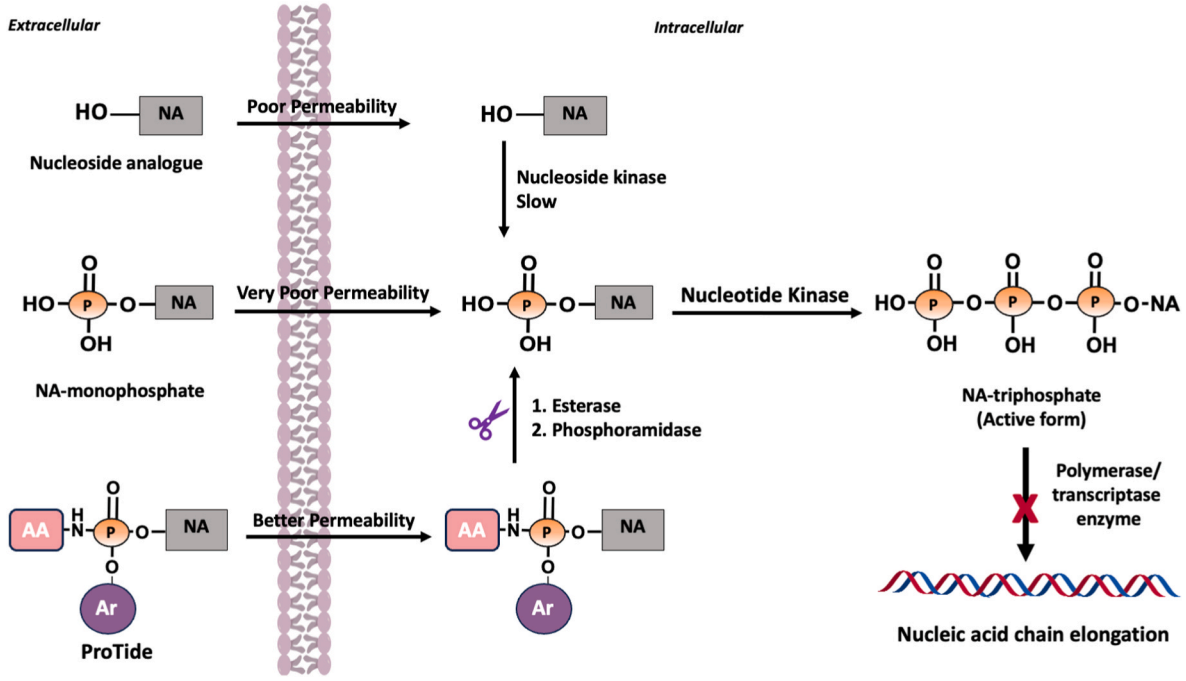

Fig. 1. Schematic representation of the cellular uptake and intracellular bioactivation of nucleoside analogues (NAs), NAs monophosphate (NAMP) and ProTides. ProTides are unmasked by host esterase and phosphoramidase type enzymes, releasing NAMP, which is further phosphorylated by cellular kinases to generate the active form of NATP which inhibits polymerase or transcriptase enzymes.

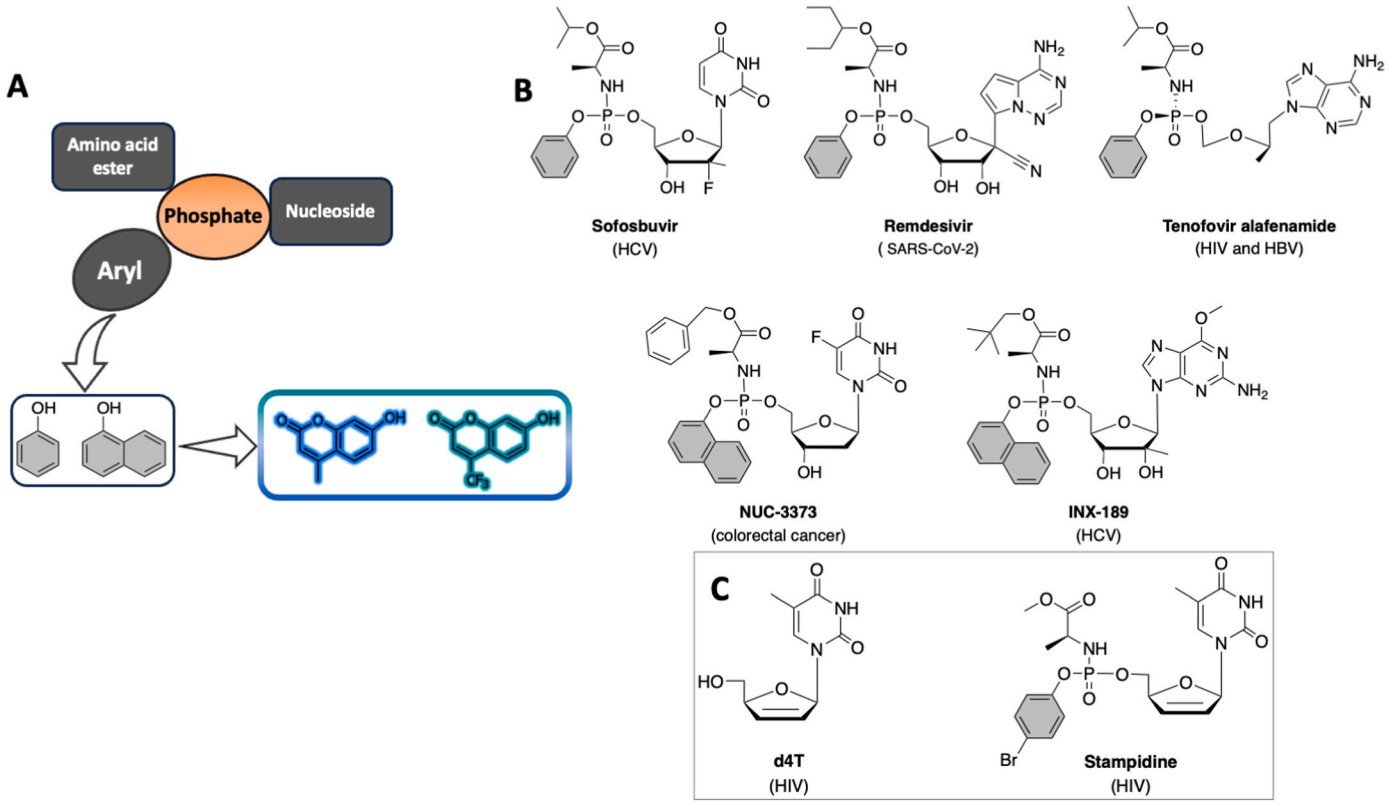

Fig. 2. (**A**) Schematic representation of the main components of a ProTide structure and the replacement of the conventional aryl group (phenyl or 1-naphthyl) with a coumarin-based component: 4MU (blue) or 4TFMU (green). (**B**) Examples of FDA approved and clinical trial candidate ProTides. (**C**) stavudine (d4T) and stampidine.

1.4. Coumarin derivatives

Coumarins are a diverse class of compounds of natural and synthetic origins, known for their chemical stability, solubility, and low toxicity, making them highly attractive scaffolds for drug development [27–30]. They exhibit a broad spectrum of biological activities, including anticancer, antimicrobial, analgesic and anti-inflammatory [27–30]. Additionally, coumarins exhibit antiviral activity against HIV, HCV, dengue, bovine viral diarrhoea, respiratory syncytial virus (RSV), influenza, herpes, HBV, chikungunya and other viruses [27,30–35].

Optimisation of coumarin scaffolds has led to clinically approved agents, such as the HIV protease inhibitor tipranavir [30] and calanolide-based analogues as HIV-1 reverse transcriptase inhibitors [36,37]. Other coumarin derivatives act as HIV inhibitors by arresting G1 phase of the cell cycle, blocking viral entry, inhibiting reverse transcriptase or interfering with viral integration [38–40]. Coumarin derivatives also serve as versatile fluorescent probes due to their cell-permeability, tuneable photophysical properties and biocompatibility, enabling applications of molecular detection and imaging in cellular studies [41–44].

4-Methylumbelliferone (4MU, hymecromone), is a coumarin derivative widely found in plants. Clinically, 4MU is prescribed in Europe and Asia for the treatment of cholestasis and biliary spasm. In addition to its hepatoprotective and anti-inflammatory properties, 4MU is commonly used as a pH-sensitive fluorescence indicator [45–47]. Its ability to inhibit hyaluronic acid synthesis was first reported in 1997 [48]. Hyaluronic acid, a major component of extracellular matrix, plays key roles in cell growth and inflammation, and is implicated in diseases such as viral transmission and tumour progression [49,50].

Numerous studies have demonstrated that 4MU inhibits the proliferation, migration and invasion of cancer cells supporting its potential as an anticancer agent [47]. Notably, 4MU has also exhibited antiviral activity and progressed to phase II clinical trials for the treatment of chronic HBV and HCV under the registered name of Heparvit [51]. Furthermore, 4MU has been proposed as a candidate for HIV-1 reservoir eradication (“shock and kill” strategies), as it can effectively reactivate latent HIV-1 with low cellular toxicity [52].

In animal models, 4MU has been shown to decrease inflammation and fibrosis, as well as reduce body weight, serum cholesterol, and insulin resistance. This broad spectrum of effects suggests that 4MU may act on multiple, yet unidentified, molecular targets [45]. The synthetic fluorinated analogue of 4MU, 4-trifluoromethylumbelliferone (4TFMU), has also been investigated. Incorporation of fluorine atoms can significantly alter a compound's physicochemical and pharmacological properties, affecting its conformation, pK_a, intrinsic potency, membrane permeability, metabolic pathways, and pharmacokinetics [16,29,53–57]. 4TFMU derivatives are utilised as fluorescent probe for imaging of the endoplasmic reticulum located carboxylesterases, enzymes responsible for the cleavage and activation of ester-containing prodrugs. 4TFMU exhibits distinct excitation and emission wavelengths, high fluorescence quantum yields, and minimal pH-dependent changes in fluorescence [58]. In literature, coumarin-based derivatives and coumarin hybrids are presented as useful scaffolds with potent anti-HIV activity [44,59,60].

1.5. Resistance development

The emergence of resistance to both antiviral and anticancer drugs, continues to pose a global health challenge [61]. In 1980s, HIV rapidly developed resistance to the first antiretroviral (ARV) drugs, limiting treatment duration to only a few months. Although current combination ARV therapies generally achieve sustained long-term viral suppression, resistance still arises in certain patient populations [62]. Nonetheless, recent advances, including long-acting formulations and agents like

lenacapavir, have significantly improved HIV treatment [63]. Similarly, relapse and resistance are major predicaments in the field of oncology, with most patients eventually developing resistance during treatment [61,64]. Elucidating the mechanisms underlying resistance to antiviral and anticancer NAs has facilitated the design of novel prodrugs, such as floxuridine and gemcitabine ProTides, as well as the development of stampidine [65,66].

1.6. Molecular hybridisation

Polypharmacology, unlike the traditional 'one drug-one target' model, involves designing compounds that act on multiple biological targets. This approach addresses the complexity of diseases, aiming for broader therapeutic effects and reduced resistance [67,68]. Similarly, molecular hybridisation (co-drug) approach, has emerged as a powerful strategy in modern medicinal chemistry, enabling the design of novel compounds by combining and covalently linking two or more pharmacophores into a single hybrid compound. This approach has gained attention for enhancing therapeutic efficacy, improving selectivity, minimising adverse effects, optimising ADMET properties and overcoming resistance by integrating complementary mechanisms of action within one molecule. Molecular hybridisation has shown promise in addressing complex diseases such as cancer, HIV, and multidrug-resistant infections, offering a versatile platform for multi-target therapy and overcoming limitations of conventional single-target agents [32,58,69,73]. In this study, we introduce the concept of using the phosphoramidate ProTide delivery system and unmasking mechanism to enable the simultaneous intracellular release of two distinct functional moieties. This hybrid mutual prodrug strategy aims to conjugate a nucleoside analogue (e.g. d4T) with a coumarin derivative (e.g. 4MU or 4TFMU) thereby integrating their therapeutic and fluorescent properties. The resulting hybrid molecule is designed to deliver dual functionality, providing therapeutic efficacy while enabling real-time mechanistic studies through intrinsic fluorescence.

2. Results and discussion

To date, phenyl or 1-naphthyl groups have been exclusively used as the aryl component in ProTide promoieties. However, *in vivo* bioactivation of these conventional ProTides produces equimolar amounts of phenol or 1-naphthol, which lack therapeutic benefit and may contribute to liver and kidney toxicity upon long-term exposure [70,71]. Phenol-containing ProTides have been associated with potential hepatotoxicity risks, as reflected in clinical safety data. For example, Acelarin (NUC-1031), a phenol-based ProTide, demonstrated a higher incidence of hepatobiliary disorders and liver injury markers in Phase III trials [72]. In contrast, 4-methylumbelliferone (4-MU), the coumarin derivative incorporated in our design, is well-documented for its hepatoprotective and antioxidant properties in preclinical studies [46,48].

In this study, the concepts of molecular hybridisation and mutual prodrug were applied to develop - for the first time - hybrid ProTides with dual function. These ProTides incorporate coumarin derivatives (4MU or 4TFMU) as the aryl moiety in the antiretroviral stavudine monophosphate prodrugs, aiming to harness both their pharmacophoric and fluorophoric properties [73,74]. This strategy is designed to enhance activity, reduce toxicity, minimise resistance, and optimise ADMET properties, while also enabling fluorescence-based mechanistic studies [75,76]. Incorporating a coumarin-based promoiety creates a single chemical entity capable of modulating multiple steps in the pathogenic cascades of complex diseases such as cancer and viral infections. Upon intracellular activation, two independent moieties are released, preserving the benefits of combination therapy within one molecule, and potentially yielding compounds with diverse biological activities [67–69]. Furthermore, the fluorescent properties of the coumarin-based ProTides enable real-time visualisation and quantification of ProTide delivery, uptake, metabolism and *in vivo* activity, as well as functional analysis of ProTide activating enzymes at the cellular level. In addition to its pharmacological and fluorescent properties, 4MU offers a more sustainable alternative to phenol or 1-naphthol, reducing environmental impact and improving synthetic safety.

2.1. Chemistry

The hybrid dual-function coumarin-based ProTides (**18**–**25**) of stavudine (d4T, **17**) were synthesised using similar procedures to the previously described phosphorochloridate chemistry in three steps, as illustrated in Scheme 1 [7,16,18]. The chromenyl phosphorodichloridate derivatives **3** and **4** were prepared from 4MU (**1**) or 4TFMU (**2**) and phosphorus oxychloride ($POCl_3$) in the presence of triethylamine (Et_3N) and monitored by ^{31}P- NMR where a single peak appears at around δ » 3 ppm. L-alanine esters are the most effective and commonly used amino acid masking group in ProTides [77,78]. Subsequent reactions with four variations of L-alanine esters; methyl (Me), ethyl (Et), isopropyl (iPr) and benzyl (Bn), (**5**–**8**) in the presence of triethylamine (Et_3N), afforded the corresponding chromenyl phosphorochloridates **9**–**16**. This reaction was also monitored by ^{31}P NMR, where two peaks corresponding to the two diastereoisomers (R_p/S_p) of the chiral phosphorus centre appeared at around δ » 7 ppm. ^{31}P NMR was used to monitor these reactions rather than TLC because of the high chemical instability of the intermediates. The ProTides were then formed by coupling the chromenyl phosphorochloridate derivatives (**9**–**16**) with stavudine nucleoside (d4T, **17**), using *tert*-butyl magnesium chloride (*t*-BuMgCl) as a hindered strong base. After stirring for 24h at ambient temperature, the crude coumarin-d4T ProTides **18**–**25** were formed and subsequently purified by flash column chromatography and preparative TLC, yielding the pure products in the characteristically low to moderate yields associated with ProTide chemistry (4–15 %) [18]. Each coumarin-d4T phosphoramidate **18**–**25** was generated as a pair of diastereomers (R_p/S_p) in approximately a 1:1 ratio, as revealed by the two closely spaced peaks in their ^{31}P NMR spectrum.

Interestingly, two additional side products were consistently observed in the crude mixtures from the final step, with ^{31}P NMR chemical shifts at $\delta \approx 8$ and 12 ppm. The signal at $\delta \approx 12$ ppm is characteristic of phosphorodiamidates (diamidates), another known class of NA monophosphate prodrugs. Two examples of this side product were successfully isolated, compounds **26** and **27**, which eluted after their corresponding coumarin ProTides, compounds **23** (EtAla, 4TFMU) and **21** (BnAla, 4MU), respectively. The identities of **26** and **27** were confirmed as diamidates through comprehensive spectral analyses including ^{1}H NMR, ^{31}P NMR, ^{13}C NMR and mass spectrometry, Scheme 1. As previously mentioned phosphorodiamidates represent another prodrug form of NAMP incorporating a natural and non-toxic amino acid ester promoiety [21–23,78].

Notably, the sequence of reactions leading to the formation of these phosphorodiamidates differs substantially from conventional methods. Traditionally, phosphorodiamidates are synthesised via phosphorylation of nucleoside analogue (NA) with $POCl_3$ to form a phosphorodichloridate intermediate (**I**), followed by the addition of an excess of amino acid ester, Fig. 3. These methods often result in low yields and, in some cases, not successful [22,23].

In contrast, our findings indicate that the addition of amino acids (**5**–**8**) to chromenyl phosphorodichloridate intermediates (**3** and **4**) generates two possible intermediates (**II** and **X**), depending on the number of amino acid ester molecules involved in the reaction. Reaction with one equivalent of amino acid ester yields a ProTide via intermediate **II**, while reaction with two amino acid ester equivalents forms a diamidate via intermediate **X**, Fig. 3.

The phosphorodiamidate product is formed through selective nucleophilic displacement/substitution of the doubly substituted coumarin derivative **X** by the 5′-hydroxyl group of stavudine (**17**, d4T) in the presence of *t*-BuMgCl as a strong base, Fig. 3. Indeed, the second side product, observed with ^{31}P NMR chemical shift at $\delta \approx 8$ was

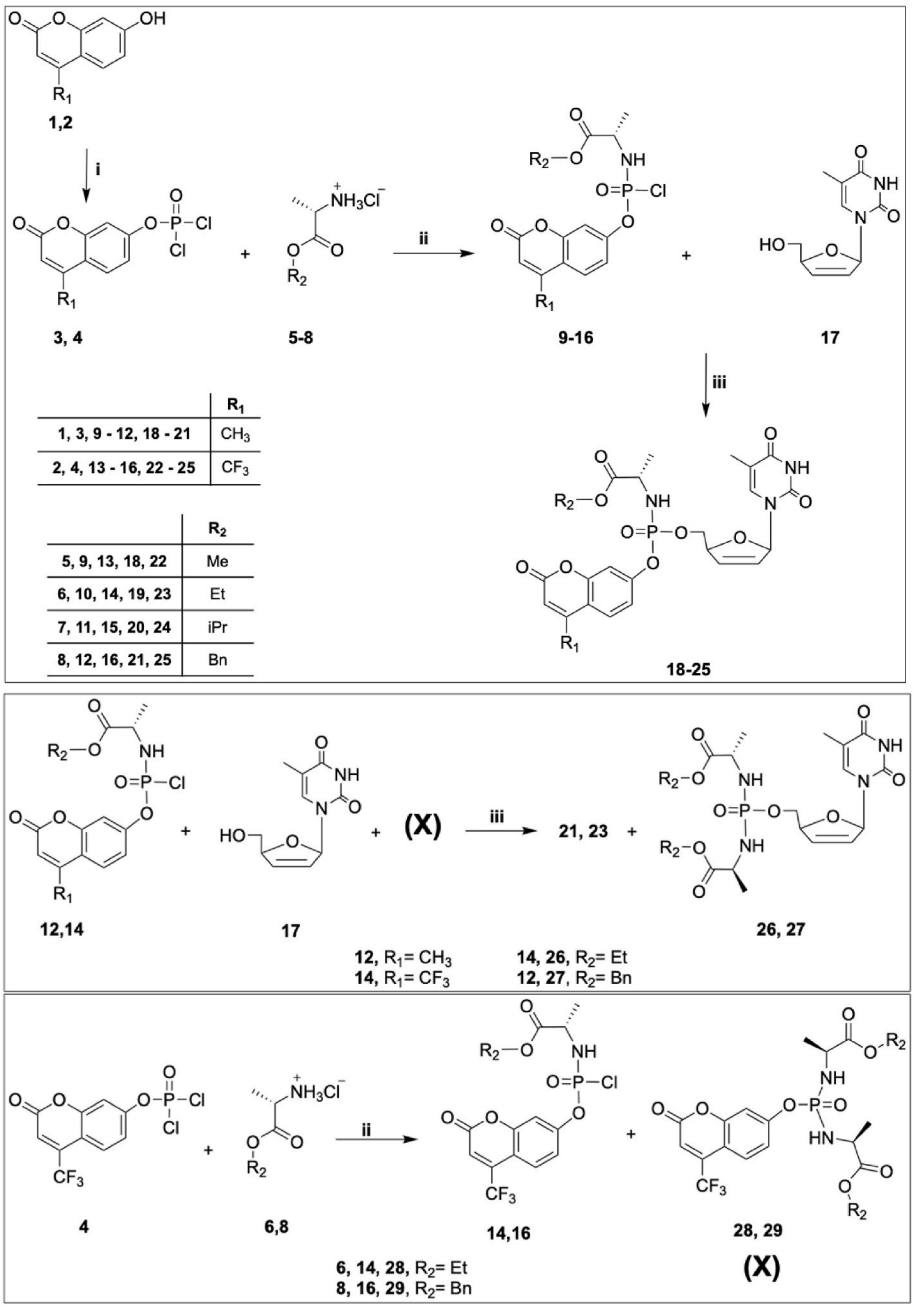

Scheme 1. Top: Synthesis of coumarin-d4T hybrid ProTides (**18**–**25**); Reagents and conditions: i) $POCl_3$, Et_3N, anhydrous Et_2O, −78 °C, 1h to rt, 1 h, ii) Et_3N, anhydrous DCM, −78 °C, 1h to rt, 1h, iii) *t*-BuMgCl, anhydrous THF, rt, 24 h, **Middle:** Serendipitous formation of phosphorodiamidates such as **26** and **27** and **Bottom:** formation of phosphorodiamidating reagents (**X**) such as **28** and **29.**

characterised as the doubly substituted compound of formula (**X** e.g. **28** and **29**) Scheme 1. These intermediates of formula **X** are chemically stable, yet sufficiently reactive to generate phosphorodiamidate, with 4MU or 4TFMU acting as good leaving groups, Scheme 1 and Fig. 3.

This serendipitously discovered synthetic route offers a promising alternative to conventional methods for preparing phosphorodiamidate (diamidate) prodrugs. Unlike traditional approaches that often suffers from low yields and unstable phosphorodichloridate intermediates, this strategy employs a novel class of chemically stable phosphorodiamidating reagents (e.g. **28** and **29**) of intermediate (**X**) formula, Scheme 1 and Fig. 3. These reagents enable direct nucleophilic displacement with activated nucleosides and non-nucleosides, facilitating more efficient synthesis and improved yields. This advancement establishes a versatile and reproducible platform for diamidate prodrug development with strong potential for scalability and broader applicability across diverse therapeutic scaffolds.

Similar displacement reactions have been reported for the diastereoselective synthesis of ProTides using pentafluorophenol or 4-nitrophenol as leaving groups. These electron-withdrawing groups enhance the reactivity of the stable phenolic phosphorylating reagents towards nucleophilic attack, in contrast to the instability of the traditional chlorophosphoramidate intermediates [79,80]. Phosphorodiamidate prodrugs mitigate issues associated with diastereomeric mixtures and the release of potentially toxic aryl moieties from ProTides, facilitating safer therapeutic development.

All products were structurally confirmed by NMR spectral analyses; ^{1}H, ^{31}P, ^{19}F and ^{13}C NMR as well as high resolution mass spectrometry.

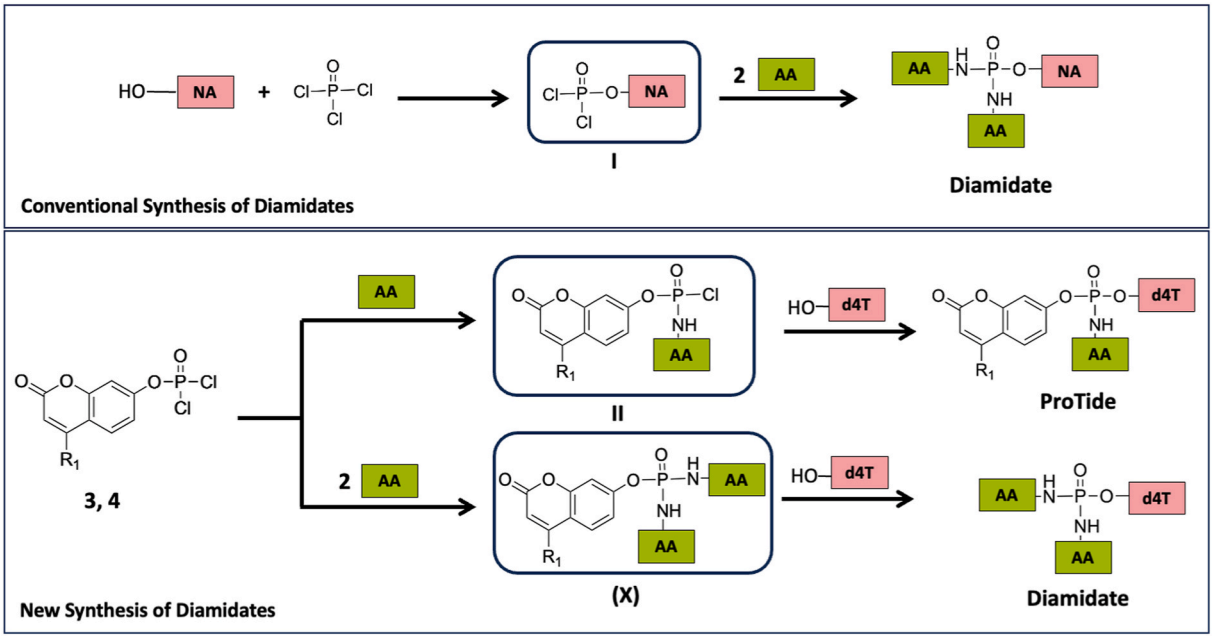

Fig. 3. Top; Conventional synthesis of diamidate via phosphorylation of NA with $POCl_3$ to form intermediate **I**, followed by addition of two amino acid (AA) molecules. **Bottom**; Addition of one AA molecule yields a ProTide via intermediate **II**, while addition of two AA molecules produces diamidate via intermediate (**X**).

2.2. Structure-activity relationship (SAR) analysis

The antiviral activity (IC_{50}) and cytotoxicity (CC_{50}) profiles of coumarin-based d4T phosphoramidate (ProTides, **18–25**) and phosphorodiamidates (diamidates, **26** and **27**) were evaluated *in vitro* against two strains of human immunodeficiency virus: HIV-1 (strain III_B), and HIV-2 (strain ROD) [81,82].

The parent compound stavudine (d4T, **17**) was used as a positive control. All tested ProTides demonstrated markedly enhanced antiviral activity compared to d4T, with IC_{50} values ranging from 0.08 to 0.22 μM (HIV-1) and 0.14 to 0.36 μM (HIV-2), versus 0.40 μM and 0.45 μM for d4T, respectively, Table 1. The only exception was ProTide **20** (iPrAla, 4MU), which showed relatively reduced activity; 0.45 μM (HIV-1) and 69 μM (HIV-2).

Within the 4MU-based ProTide series (**18–21**), the antiviral activity followed the order of Bn > Et ≈ Me > iPr, while the 4TFMU-based series (**22–25**) showed comparable potencies. The ethyl and methyl esters of L-alanine in 4MU-based ProTides exhibited similar activity, as expected, given their comparable properties. In contrast, the isopropyl ester was the least active, likely due to its slower hydrolysis rate, which can impede efficient release of the active monophosphate. The L-alanine benzyl ester is frequently employed in ProTide design because of its favourable balance of lipophilicity and enzymatic activation [18,65]. Overall, ProTides bearing the 4MU aryl motif exhibited better antiviral activity compared to their 4TFMU counterparts. The most potent compound was ProTide **21** (BnAla, 4MU), with IC_{50} values of 0.08 μM (HIV-1) and 0.14 μM (HIV-2), representing a more than fourfold improvement over d4T, Table 1 and Fig. 4.

Between the diamidates, compound **26** (2EtAla) showed better activity than d4T, but was slightly less active than the corresponding coumarin ProTides **19** (EtAla, 4MU) and **23** (EtAla, 4TFMU). In contrast, diamidate **27** (2BnAla) was nearly twice as active as **26** and exhibited potency intermediate between ProTides **21** (BnAla, 4MU) and **25** (BnAla, 4TFMU), **21** > **27** > **25**. Another key parameter, the selectivity index (SI; CC_{50}/IC_{50}), is summarised in Table 1 and Fig. 4. All compounds showed higher SI values against HIV-1 than HIV-2, except for ProTide **19**. This trend is consistent with previous reports on ProTide-based nucleoside analogues [16]. One possible explanation is the structural differences between HIV-1 and HIV-2 reverse transcriptase, which may influence substrate recognition and incorporation efficiency of the released nucleotide. Generally, 4MU-based ProTides had better SI values than their 4TFMU counterparts, except for ProTide **24** (iPrAla,

Table 1
Antiviral activity (IC_{50}), toxicity (CC_{50}) and selectivity index (SI) of stavudine (d4T, **17**), coumarin-based ProTides (**18–25**) and phosphorodiamidates (**26** and **27**) against HIV-1 (strain III_B) and HIV-2 (strain ROD), n = 3.

ID	HIV-1 (III_B_MT-4)			HIV-2 (ROD_MT-4)		
	IC_{50} (μM) ± SD	CC_{50} (μM) ± SD	SI	IC_{50} WT (μM) ± SD	CC_{50}(μM) ± SD	SI
17 (d4T)	0.40 ± 0.09	312 ± 7	790	0.45 ± 0.09	312 ± 7	703
18	0.22 ± 0.09	115 ± 2	525	0.27 ± 0.18	115 ± 2	421
19	0.19 ± 0.09	88 ± 3	450	0.14 ± 0.05	87.7 ± 3	609
20	0.45 ± 0.07	167 ± 2	372	0.69 ± 0.33	168 ± 2	243
21	0.08 ± 0.03	130 ± 4	1549	0.14 ± 0.08	130 ± 4	923
22	0.20 ± 0.03	46 ± 2	232	0.35 ± 0.10	46 ± 2	132
23	0.19 ± 0.02	44 ± 6	228	0.31 ± 0.06	44 ± 6	143
24	0.21 ± 0.03	149 ± 3	727	0.36 ± 0.03	150 ± 3	416
25	0.19 ± 0.03	59 ± 2	309	0.25 ± 0.03	59 ± 2	236
26	0.29 ± 0.14	199 ± 2	686	0.40 ± 0.08	199 ± 2	500
27	0.14 ± 0.06	164 ± 1	1214	0.18 ± 0.08	164 ± 1	936
1 (4MU)	>515.13	>515	<1	>515.13	91 ± 6	<1
2 (4TFMU)	>76.78	77 ± 1	<1	>76.78	77 ± 1	<1

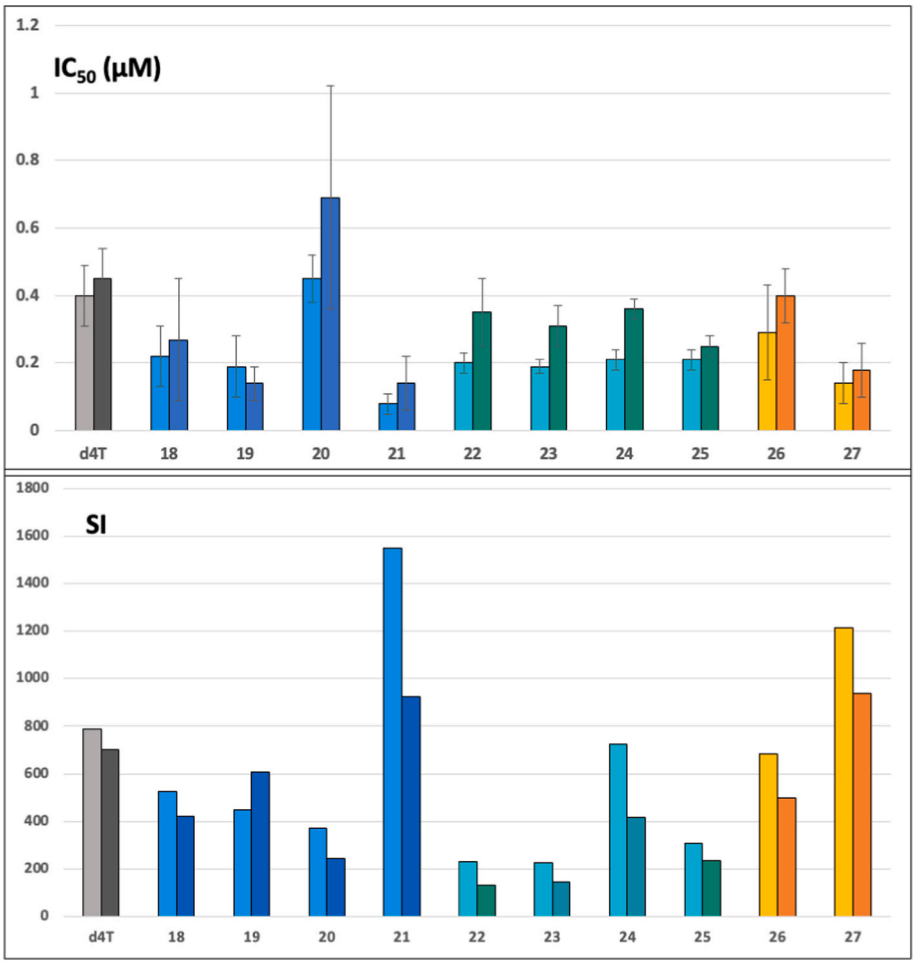

Fig. 4. (**Top**) Antiviral activity (IC_{50}, μM± SD); (**Bottom**) Selectivity index (SI), of stavudine (d4T, grey), 4MU-based ProTides (**18**–**21, blue**), 4TFMU-based ProTides (**22**–**25, turquoise**) and phosphorodiamidates (**26** and **27, orange**) against HIV-1 (left) and HIV-2 (right).

4TFMU), which outperformed its 4MU counterpart, ProTide **20**. The most favourable SI was observed for ProTide **21**, with values of 1549 (HIV-1) and 923 (HIV-2), followed by diamidate **27**. Diamidate **26** and ProTide **24** had SI values comparable to each other, but both were slightly lower than that of d4T.

In summary, ProTide **21** emerged as the most promising candidate, combining potent antiviral activity with minimal cytotoxicity, making it a good lead for further development.

To determine whether the hybrid ProTides function as prodrugs it is important to investigate whether the nucleotide analogues are degraded to their parent nucleoside to be subsequently rephosphorylated or if they possess the ability to bypass the first phosphorylation step by cellular thymidine kinase (TK) and be converted to their di- and triphosphate, Fig. 1. Therefore, we compared their antiviral activities against HIV-1 (strain III_B) in both wild-type C8166 and mutant TK-deficient C8166-TK^- cells. In wild-type cells (C8166), all compounds demonstrated 4–80 fold enhanced activity compared to stavudine (d4T). d4T completely lost its activity in C8166-TK^- cells, consistent with its dependence on TK-mediated phosphorylation. In contrast, several ProTides retained significant activity in the TK-deficient cell line, indicating their ability to bypass the TK-dependent activation step. These included three out of four 4MU-based ProTides, **19**, **20** and **21**, two out of four 4TFMU-based ProTides, **24** and **25,** and diamidate **27**, which confirm that these compounds do not require TK for activation. Although ProTide **23** showed the highest activity in the wild type cells ($IC_{50} = 0.05$ μM), it was ProTide **21** that exhibited the best activity in TK-deficient cells ($IC_{50} =$ 0.06 μM), where d4T was completely inactive. The above findings highlight 4MU-d4T ProTide **21** as a particularly promising candidate, followed by 4TFMU-d4T Protide **25** and diamidate **27**, for further development of anti-HIV therapies independent from TK expression. Notably, all three compounds share a benzyl alanine ester as a common structural feature, which may contribute to their enhanced cellular potency in C8166-TK^- cells. Table 2.

These results strongly suggest that the tested compounds successfully deliver the d4T monophosphate intracellularly, thereby bypassing the

Table 2
Antiviral activity (IC_{50}, μM) of target compounds against HIV-1 (strain III_B) in wild-type C8166 cells and thymidine kinase-deficient C8166-TK^- cells, compared to stavudine (d4T), n = 3. NA: not active.

ID	HIV-1 (III_B)	
	IC_{50} (μM ± SD) in C8166 cells	IC_{50} (μM ± SD) in C8166-TK^- cells
d4T	4.06 ± 0.18	NA
18	0.53 ± 0.33	≥0.64
19	0.28 ± 0.00	1.63 ± 1.19
20	0.97 ± 0.83	1.37 ± 0.05
21	0.19 ± 0.02	0.06 ± 0.02
22	0.17 ± 0.13	≥0.28
23	0.05 ± 0.02	≥0.19
24	0.41 ± 0.25	0.35 ± 0.22
25	0.22 ± 0.03	0.11 ± 0.01
26	0.28 ± 0.04	≥1.41
27	0.30 ± 0.05	0.32 ± 0.05
1	NA	NA
2	NA	NA

rate-limiting phosphorylation step mediated by thymidine kinase (TK). This TK-independent activation mechanism leads to enhanced cellular potency, as evidenced by the retained antiviral activity in TK-deficient cells.

The observed lack of antiviral activity of 4MU and 4TFMU in our bioassay experiments may be attributed to poor cellular permeability, which limits their intracellular concentration. This hypothesis is supported by pharmacokinetic studies showing that 4MU has very low oral bioavailability with an area under curve (AUC) ratio of 96:1 for intravenous versus oral administration in mice, indicating limited absorption and permeability [49]. Its low aqueous solubility and limited solubility in organic solvents further contribute to restricted passive diffusion across cell membranes. While specific data for 4TFMU are limited, its structural similarity to 4MU suggests similar limitations. However, incorporation of these moieties into ProTide scaffolds, could enhance cellular uptake and overcome permeability barriers. This supports the rationale for using ProTide conjugation as mutual prodrug not only to mask the NA monophosphate group but also to enhance intracellular delivery of otherwise impermeable pharmacophoric/fluorophoric aryl groups. Future studies are warranted to systematically investigate the cellular uptake and permeability profiles of 4MU and 4TFMU in both free and ProTide-conjugated forms.

2.3. Enzymatic activation of ProTide 19

The enzymatic bioactivation of ProTides is essential for their activity. Upon cleavage of the two promoiety motifs, the nucleoside monophosphate is released and subsequently phosphorylated to its di- and triphosphate form which inhibits viral replication.

Previous studies have described a multi-step intracellular activation pathway for ProTides. This begins with hydrolysis of the amino acid ester by a carboxyesterase type enzyme, forming intermediate **A**. This intermediate undergoes spontaneous cyclisation, resulting in the loss of the aryl moiety via internal nucleophilic attack of the carboxylate residue on the phosphorus centre, yielding intermediate **B**. The unstable cyclic mixed anhydride is then hydrolysed to release intermediate **C**, an alanine metabolite. A phosphoramidase-type enzyme, subsequently cleaves the P–N bond, releasing the nucleoside monophosphate **D**, which is trapped intracellularly due to its polar phosphate group and undergoes further phosphorylation to the active triphosphate form. Figs. 1 and 5 [16,18,83–85].

However, not all ProTides follow this bioactivation route. In some cases, enzymatic metabolism leads to dephosphorylation, releasing the inactive free nucleoside instead [86].

To determine whether a ProTide follows the proposed activation pathway, it is incubated with carboxypeptidase enzyme and its ^{31}P NMR chemical shifts are monitored over time to track changes in the phosphorus chemical environment. For ProTides containing fluorine, ^{19}F NMR can be employed as a complementary technique to observe chemical shift variations, providing additional evidence of structural changes during enzymatic activation [16]. ProTide **19** was incubated with carboxypeptidase Y, and the reaction progress was monitored using ^{31}P NMR spectroscopy. ProTide **19** (5 mg) was dissolved in acetone–d_6 (0.15 mL) with Trizma buffer (0.3 mL, pH 7.6). The ^{31}P NMR of this mixture was recorded as control experiment which showed two peaks at δ 3.40 and 3.58 ppm, corresponding to the two diastereoisomers of ProTide **19**. Upon addition of carboxypeptidase Y (0.1 mg in 0.15 mL Trizma) a new peak at $\delta \approx 6.60$ ppm appeared within 7 min corresponding to the formation of the achiral intermediate **C**. The increasing intensity of this peak over time indicated the accumulation of a stable product, confirming that ProTide **19** is enzymatically cleavable, and that activation is successfully initiated by carboxypeptidase Y, leading to the release of its unmasked monophosphate form, Fig. 5.

2.4. Fluorescent properties of hybrid ProTides

Fluorescent probes are widely employed to track the release of biologically active compounds by exciting electrons with a beam of light (excitation), which then emit light at a different wavelength (emission) [41]. Among these, 4MU and 4TFMU are notable for their strong fluorescent properties. In our target ProTides, the aryl moieties of 4MU and 4TFMU serve not only as masking groups but also as fluorescent probes, offering a valuable opportunity to study ProTide activation pathways in greater detail. This approach enables real-time monitoring by detecting the release of a highly fluorescent reporter molecule from its non-fluorescent profluorophore ProTide.

In a preliminary study, fluorescence intensities of 100 μM methanolic solutions of 4MU and 4MU-based ProTides were measured at an excitation wavelength (λ_{Ex}) of 412 nm and an emission wavelength (λ_{Em}) of 421 nm, Fig. 6. Under these conditions, ProTides (e.g. **18–20**) exhibited

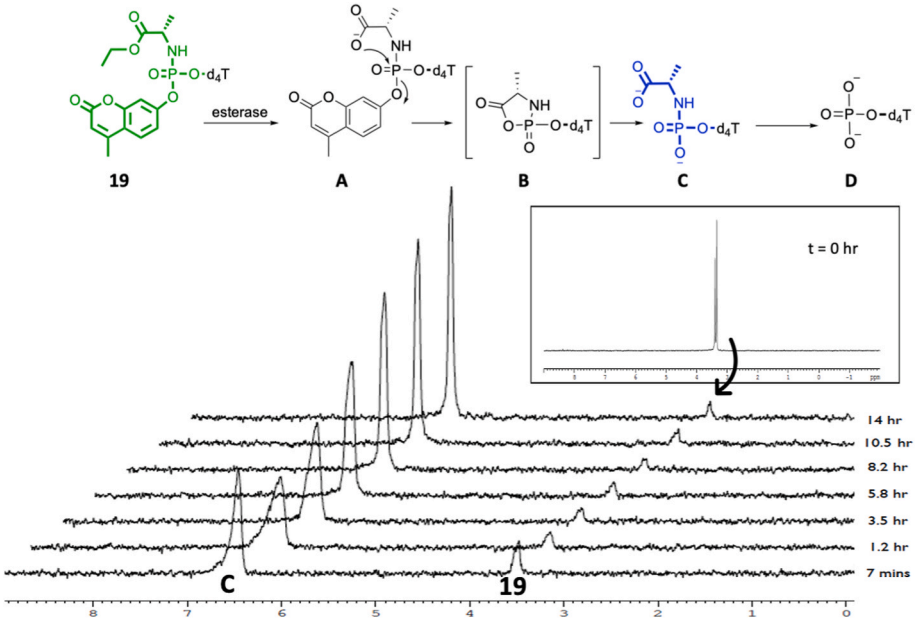

Fig. 5. ^{31}P NMR spectra of ProTide **19** following incubation with carboxypeptidase Y. The initial spectrum shows two peaks corresponding to the diastereoisomers of ProTide **19** at $\delta = 3.40$ and 3.58 ppm. Within 7 min of incubation a new peak emerges at $\delta = 6.60$ ppm indicating the formation of intermediate **C.**

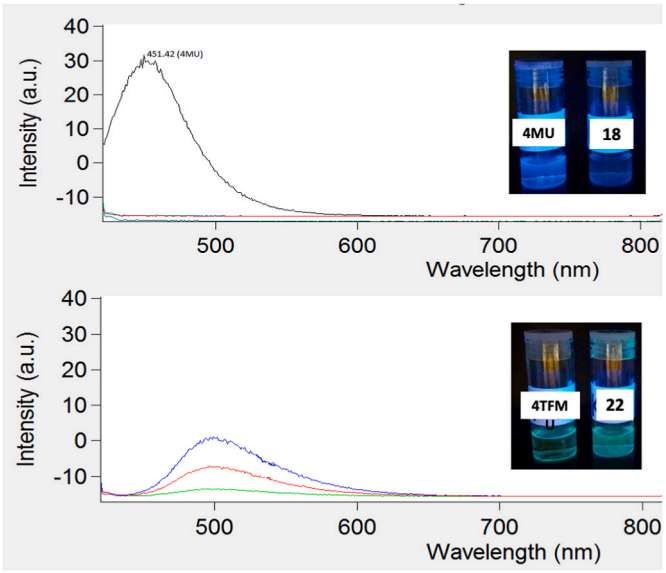

Fig. 6. Emission spectra at λ_{Ex} of 412 nm and λ_{Em} of 421 nm of 100 μM methanolic solutions of (**Top**) 4MU (black), ProTides **18** (red), **19** (blue), **20** (green). **(Top right)** 4MU and **18** under long-wave UV light (366 nm). **(Bottom)** 4TFMU (blue), ProTides **22** (green) and **23** (red). **(Bottom right)** 4TFMU and **22** under long-wave UV light (366 nm).

no fluorescence, indicating that they act as profluorophores, non-fluorescent (switched off) precursors until activated. Upon enzymatic cleavage, the release of the parent 4MU moiety effectively switches the fluorescence on, acting as a fluorophore. This was visually confirmed under a long-wave UV lamp (366 nm), where ProTide **18** lacked the characteristic blue fluorescence of the parent 4MU, consistent with its switched off state, Fig. 6. In contrast, 4TFMU-based ProTides (e.g. **22**, **23**) exhibited a significant reduction in fluorescence intensity relative to the parent 4TFMU, though not a complete loss, when measured under the same conditions at ($\lambda_{Ex} = 412$ nm and $\lambda_{Em} = 421$ nm) in methanol.

These results confirm that coumarin-based ProTides and their corresponding coumarin parent compounds possess distinct fluorescence profiles. This distinction can be employed to investigate ProTide cellular uptake, metabolism, and activation using fluorescence-based assays. The unique fluorescence characteristics of these compounds are promising and suggest potential for developing sensitive and selective methods to monitor ProTide behaviour in biological systems. However, these are preliminary results, and further investigations are warranted to optimise experimental conditions such as excitation and emission parameters, pH values and solvent systems, to enhance the reliability and sensitivity of fluorescence detection of these profluorophore ProTides.

2.5. ADMET properties

Pharmacokinetic properties including absorption, distribution, metabolism, excretion, and toxicity (ADMET) can be predicted *in silico* based on the chemical structure of the proposed therapeutic agent [87]. SwissADME is an online tool that calculates physicochemical descriptors and predicts ADME related properties of small molecules [87,88]. In this study, SwissADME was used to evaluate the pharmacokinetic profiles of the target compounds (**18**–**27**), Table 3.

One of the key descriptors is the consensus $logP_{o/w}$ (cons logP), which represents the average of log P values predicted by five different methods. All compounds (**18**–**27**) showed cons logP values below 5 in accordance with Lipinski's rule of five, indicating acceptable lipophilicity. Among the compounds, ProTides (**18**–**25**) were generally more lipophilic than diamidates (**26** and **27**). Furthermore, 4TFMU-based ProTides (**22**–**25**) were more lipophilic than their 4MU counterparts (**18**–**21**), consistent with the known lipophilic nature of the trifluoromethyl group, Table 3. The Topological Polar Surface Area (TPSA), measured in $Å^2$, was slightly higher for ProTides (**18**–**25**) compared to diamidates (**26** and **27**), Table 3. Gastrointestinal (GI), which is an estimate of the likelihood of passive absorption by the GI tract, was predicted to be low for all prodrugs (**18**–**27**). In contrast, d4T, 4MU, 4TFMU, phenol and 1-naphthol were predicted to have high GI absorption. The blood-brain barrier (BBB) permeability indicated that none of the prodrugs (**18**–**27**), nor d4T are likely to penetrate the BBB. However, 4MU and 4TFMU, phenol and 1-naphthol were predicted to have potential for BBB penetration, Table 3. Additionally, the bioavailability score, which estimates the probability of achieving at least 10 % oral bioavailability in rats or measurable permeability in Caco-2 cells, was lower for all prodrugs (**18**–**27**) compared to the non-prodrug compounds, Table 3.

According to the SwissADME, all target compounds (**18**–**27**) exhibit consensus logP values below 5, low GI absorption and no BBB permeability, in contrast to the free small molecules d4T, 4MU, 4TFMU, phenol, and 1-naphthol, which scored higher in both GI and BBB permeability. Bioavailability scores were lower for ProTides and diamidates (**18**–**27**) compared to non-prodrug compounds, suggesting limited oral absorption. However, the predicted ADMET profiles of the hybrid ProTides are similar to the FDA approved ProTides; sofosbuvir and remdesivir, Table 3. Overall, these findings suggest that the incorporation of 4MU or 4TFMU into ProTide scaffolds offer the opportunity to modulate pharmacokinetic properties compared to the traditional

Table 3
Pharmacokinetic prediction of selected ADMET parameters for d4T, 4MU, 4TFMU, phenol, 1-naphthol, target compounds **18**–**27** and FDA approved ProTides; sofosbuvir and remdesivir (calculated by SwissADME).

ID	MW	Cons logP	TPSA $Å^2$	GI absorption	BBB permanent	Bioavailability score
d4T	224.21	−0.04	84.32	High	No	0.55
4MU	176.17	1.81	50.44		Yes	
4TFMU	230.14	2.53	50.44			
Phenol	94.11	1.41	20.23			
1-Naphthol	144.17	2.43	20.23			
18	547.45	1.81	177.97			
19	561.48	2.07				
20	575.50	2.32				
21	623.55	2.74				
22	601.42	2.45	177.97	Low	No	0.17
23	615.45	2.76				
24	629.48	3.01				
25	677.52	3.52				
26	502.46	0.70	176.86			
27	626.59	2.25				
Sofosbuvir	529.45	1.40	167.99			
Remdesivir	588.55	1.40	213.36			

aryl groups, phenol and 1-naphthol, Table 3.

Fig. 7 illustrates the SwissADME predicted oral bioavailability of six compounds; d4T, 4MU, 4TFMU**, 21, 25,** and **27**, based on their placement within a coloured zone that represents the optimal physicochemical space for oral bioavailability. This zone is defined by the following criteria: Lipophilicity (LIPO), Size (MW), Polarity (POLAR), Insolubility (INSOLU), Insaturation (INSATU), Flexibility (FLEX).

The predicted optimal criteria are LIPO (Lipophilicity): $-0.7 <$ XLOGP3 $< +5.0$, SIZE: 150 g/mol $<$ MW $<$ 500 g/mol, POLAR (Polarity): 20 $Å^2 <$ TPSA $<$130 $Å^2$, INSOLU (Insolubility): $-6 <$ Log S (ESOL) < 0. INSATU (Insaturation): 0.25 $<$ Fraction $Csp^3 < 1$, FLEX (Flexibility): 0 $<$ Number of rotatable bonds $<$9.

Compounds inside the coloured zone meet all the criteria and are predicted to have good oral bioavailability. Compounds outside the zone violate one or more criteria and are predicted to have poor or suboptimal oral bioavailability. While compounds outside the coloured zone may violate one or more criteria of predicted oral bioavailability, this does not necessarily preclude their therapeutic potential. ProTides are designed as prodrugs to enhance intracellular delivery and bypass metabolic bottlenecks. As a result, their physicochemical properties may fall outside the optimal range for oral bioavailability, yet they can still demonstrate potent activity and clinical efficacy e.g. sofosbuvir and remdesivir. Nevertheless, a comprehensive evaluation of biosafety, pharmacokinetics, and therapeutic efficacy of these compounds in appropriate animal models are needed in future studies as part of preclinical development.

3. Conclusion

This study introduces the novel incorporation of coumarins (4MU or 4TFMU) into hybrid ProTide scaffolds, replacing traditional aryl groups namely phenol and 1-naphthol, using stavudine (d4T) as a model nucleoside. This structural innovation offers multiple potential advantages, including enhanced activity, reduced toxicity, and integrated fluorescent functionality for metabolic tracking while enabling fine tuning of pharmacokinetic (ADMET) properties. Antiretroviral evaluation of our hybrid ProTides confirmed potent activity with high selectivity indices and TK-independent activation in cellular assays. Furthermore, the serendipitous isolation of phosphorodiamidates revealed an efficient synthetic route to this conventionally challenging class of prodrugs. Collectively, these findings expand the nucleoside and non-nucleoside ProTide framework by introducing multifunctional hybrid scaffolds, offering practical opportunities for developing potent, trackable, and synthetically accessible chemotherapeutic agents. Future research will focus on (i) extending this concept to other therapeutic nucleosides and non-nucleosides as well as phenol-based therapeutic agents, (ii) optimising the novel synthetic route for phosphorodiamidate prodrugs to improve yield and scalability, and (iii) establishing fluorescence calibration protocols to enable quantitative metabolic tracking. These directions will accelerate translational potential and broaden the clinical applicability of this approach.

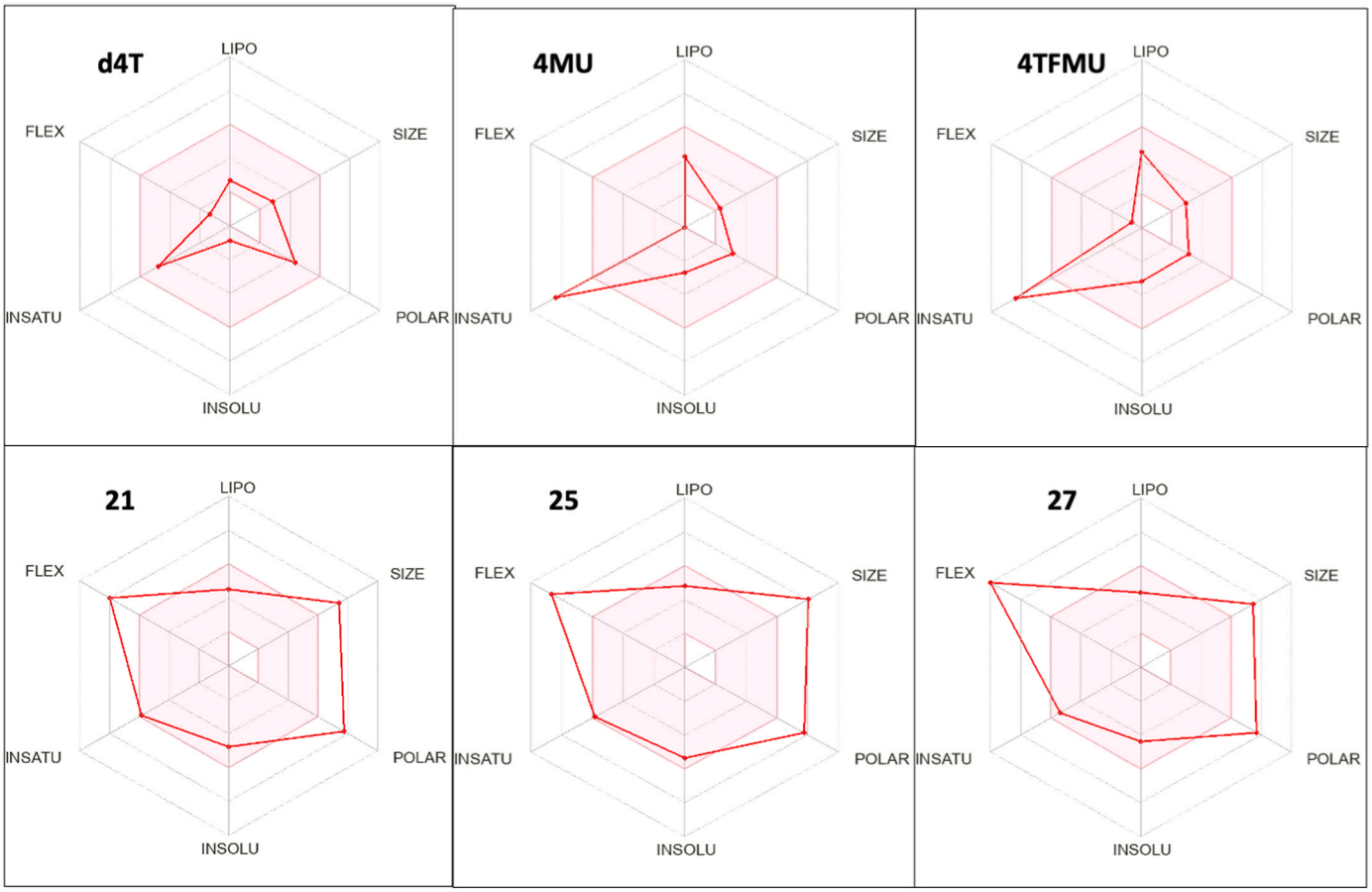

Fig. 7. Coloured zone is the suitable physicochemical space for oral bioavailability of d4T, 4MU, 4TFMU and compounds **21**, **25** and **27**. LIPO (Lipophilicity), POLAR (Polarity), INSOLU (Insolubility), INSATU (Insaturation) and FLEX (Flexibility): 0 $<$ Number.

4. Experimental section

4.1. Chemistry

4.1.1. General experimental details

All commercially available solvents and reagents were purchased from Sigma Aldrich or Carbosynth and required no further purification. Analytical TLC was conducted using pre-coated aluminium-backed plates (0.2 mm silica gel 60 with fluorescent indicator) and visualised under short-wave and long-wave UV light, at 254 and 366 nm, respectively. Preparatory TLC was conducted using Analtech Uniplate pre-coated glass-backed plates (1000 μm silica gel). Purification by flash gradient column chromatography on silica gel 35–70 μm, used mobile phase chloroform/methanol, 100/0 to 96/4. ^{31}P NMR was used to monitor both phosphorodichloridate and phosphorochloridate intermediate reactions. ^{31}P NMR (202 MHz), ^{1}H NMR (500 MHz), ^{13}C NMR (125 MHz) and ^{19}F NMR (470 MHz) spectra were used to analyse the final compounds and were recorded on a Bruker Avance 500 MHz Spectrometer and were calibrated to the residual signal of the deuterated solvent used; ($CDCl_3$). Chemical shifts (δ) were recorded as parts per million (ppm), and the following abbreviations used in the description of NMR signals: singlet (s), broad singlet (bs), doublet (d), doublet of doublet (dd), triplet (t), doublet of triplet (dt), quartet (q), and multiplet (m), and coupling constants (*J*) in Hertz (Hz). MS was performed in the EPSRC UK National Mass Spectrometry Facility, College of Medicine, Swansea University and the School of Pharmacy and Pharmaceutical Sciences, Cardiff University, both using the electrospray ionisation (ESI) method.

4.1.2. Standard procedure A: synthesis of chromenyl phosphorodichloridates (3 and 4)

To the appropriate coumarin derivative **1** or **2**, (1 mol/eq), anhydrous diethyl ether was added under a nitrogen atmosphere and stirred at room temperature (rt) for 10 min (min). Phosphorus oxychloride (1 mol/eq) was added to the reaction mixture, and then stirred at −78 °C whilst triethylamaine Et_3N (1 mol/eq) was added dropwise. The reaction mixture was left under stirring at - 78 °C for 1 h (h), then at rt for 1h. Formation of the desired phosphorodichloridate (**3**, **4**) intermediate was monitored by ^{31}P NMR. After confirmation of the production of the desired phosphorodichloridate, the Et_3N hydrochloride precipitate was filtered out under a nitrogen atmosphere, and diethyl ether solvent removed by evaporation *in vacuo*. The product was dried *in vacuo and* stored under nitrogen in the freezer.

4.1.3. Standard procedure B: synthesis of chromenyl phosphorochloridates (9–16)

To a stirred solution of the appropriate phosphorodichloridate **3** or **4** (1 mol/eq) and appropriate L-alanine ester **5**–**8** (1 mol/eq) in anhydrous DCM, Et_3N (2 mol/eq) was added dropwise at −78 °C under a nitrogen atmosphere. Following this addition, the reaction mixture was left under stirring at −78 °C for 1 h, then at rt for 1 h. Formation of the desired phosphorochloridate intermediate was monitored by ^{31}P NMR. After confirmation of the production of the desired phosphorochloridate (**9**–**16**), the Et_3N hydrochloride salt was triturated with anhydrous diethyl ether. The precipitate was filtered out under a nitrogen atmosphere, anhydrous DCM solvent removed by evaporation *in vacuo*, and product dried *in vacuo*.

4.1.4. Standard procedure C: synthesis of ProTides (18–25)

To a stirring solution of d4T (**17**, 1 mol/eq) in anhydrous THF under a nitrogen atmosphere, *t*-BuMgCl (1.1 mol/eq) was added, and stirred for 10 min. The appropriate phosphorochloridate **9**–**16** (1.2 mol/eq) dissolved in anhydrous THF was added to the reaction mixture dropwise. The reaction mixture was left under stirring at rt for 24 h, then anhydrous THF solvent removed by evaporation *in vacuo* at 25 °C. The crude product was purified by flash gradient column chromatography, eluting with increasing solvent polarity chloroform/methanol from 100/0 to 96/4. Followed by preparatory TLC using mobile phase mixture of methanol/chloroform (2/98) to isolated pure compounds.

4.1.5. Methyl(((5-(5-methyl-2,4-dioxo-3,4-dihydropyrimidin-1(2H)-yl)-2,5-dihydrofuran-2-yl)methoxy)((4-methyl-2-oxo-2H-chromen-7-yl)oxy) phosphoryl)alaninate (18, pale yellow solid, yield 10 %)

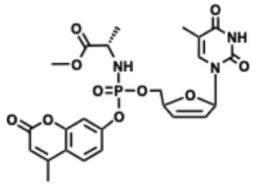

^{1}H NMR ($CDCl_3$, 500 MHz): δ 8.94 (bs, 1H, N*H*), 7.58 (dd, $J = 2$, 9 Hz, 1H, Ar*H*), 7.25-7.16 (m, 3H, Ar*H*), 7.04, 7. 02 (2s, 1H, *H*-1′), 6.40, 6.35 (2d, $J = 6$ Hz, 1H, *H*-3′), 6.26 (s, 1H, Ar*H*), [(5.97, d, $J = 5$ Hz, isomer A), (5.94, d, $J = 6$ Hz, isomer B) 1H, *H*-2'], 5.08, 5.06 (2s, 1H, *H*- 4′), 4.44-4.28 (m, 2H, *H*-5′), 4.14-3.99 (m, 2H, N*H*, C*H* ala), 3.75, 3.74 (2s, 3H, CH_3 ester), 2.44 (s, 3H, CH_3 coum), 1.87, 1.82 (2s, 3H, CH_3 nuc), 1.42, 1.38 (2d, $J = 7$ Hz, 3H, CH_3 ala). ^{31}P NMR ($CDCl_3$, 202 MHz): δ 3.15, 2.46. ^{13}C NMR ($CDCl_3$, 125 MHz): δ [(173.92, d, $^{3}J_{C\text{-}P} = 6.25$ Hz, isomer A), (173.77, d, $^{3}J_{C\text{-}P} = 7.5$ Hz, isomer B) *C*═O], 163.68, 163.64 (*C*═O 4-Nuc), 160.44, 160.39 (*C*═O coum), 154.34 (Ar*C*), [(152.91, d, $^{2}J_{C\text{-}P} = 5$ Hz, isomer A), (152.74, d, $^{2}J_{C\text{-}P} = 6.25$ Hz, isomer B) Ar*C*], 151.95, 151.90 (Ar*C*), 150.75 (*C*═O 2-Nuc), 135.75, 135.55 (Ar*C*H), 133.22, 132.85 (*C*-3′), 127.75, 127.60 (*C*-2′), 125.93, 125.88 (Ar*C*H), 117.33, 117.25 (Ar*C*), 116.75, 116.54 (2d, $^{3}J_{C\text{-}P} = 5$ Hz, Ar*C*H), 114.32, 114.27 (Ar*C*H), 111.39, 111.23 (Ar*C*), [(108.86, d, $^{3}J_{C\text{-}P} = 5$ Hz, isomer A), (108.64, d, $^{3}J_{C\text{-}P} = 6.25$ Hz, isomer B) Ar*C*H], 89.99, 89.69 (*C*-1′), 84.56, 84.49 (*C*-4′), 67.53, 66.86 (2d, $^{2}J_{C\text{-}P} = 5$ Hz, *C*-5'), 52.75, 52.72 (*C*H$_3$ ester), 50.24, 50.14 (2d, $^{2}J_{C\text{-}P} = 1.9$ Hz, *C*H ala), 20.94, 20.86 (2d, $^{3}J_{C\text{-}P} = 5$ Hz, *C*H$_3$ ala), 18.71 (*C*H$_3$ coum), 12.39, 12.34 (*C*H$_3$, Nuc). MS [ESI, *m/z*]: 570.12 [M+Na]. MS [ESI, *m/z*]: HRMS calcd for $C_{24}H_{26}N_3O_{10}P$ [M+H], 548.1429; found, 548.1417.

4.1.6. Ethyl (((5-(5-methyl-2,4-dioxo-3,4-dihydropyrimidin-1(2H)-yl)-2,5-dihydrofuran-2-yl)methoxy)((4-methyl-2-oxo-2H-chromen-7-yl)oxy) phosphoryl)alaninate (19, pale yellow solid, yield 10 %)

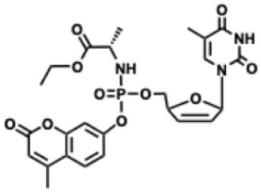

^{1}H NMR ($CDCl_3$, 500 MHz): δ 8.70, 8.65 (2s, 1H, N*H*), 7.60-7.56 (2 m, 1H, Ar*H*), [(7.30, q, $J = 1.5$ Hz, isomer A), (7.24, q, $J = 1$ Hz, isomer B), 1H, Ar*H*], 7.23-7.17 (m, 2H, Ar*H*), 7.06- 7.01 (2 m, 1H, *H*-1′), [(6.40, dt, $J = 1.5$, 6 Hz, isomer A), (6.35, dt, $J = 2$, 6 Hz, isomer B), 1H, *H*-3'], 6.28-2.26 (m, 1H, Ar*H*), 5.98, 5.95 (2dq, $J = 1.5$, 6 Hz, 1H, *H*-2′), 5.10-5.04 (m, 1H, *H*-4′), 4.45-4.29 (m, 2H, *H*-5′), 4.25-4.14 (m, 2H, CH_2 ester), 4.06-3.92 (m, 2H, N*H*, C*H* ala), 2.44 (d, $J = 1$ Hz, 3H, CH_3 coum), 1.87, 1.83 (2d, $J = 1$ Hz, 3H, CH_3 nuc), 1.41, 1.39 (2d, $J = 6.5$ Hz, 3H, CH_3 ala), 1.28, 1.27 (2t, $J = 7.5$ Hz, 3H, CH_3 ester). ^{31}P NMR ($CDCl_3$, 202 MHz): δ 3.13, 2.51. ^{13}C NMR ($CDCl_3$, 125 MHz): δ 172.79 (*C*═O ester), 162.98, 162.95 (*C*═O 4-nuc), 159.84, 159.80 (*C*═O coum), 153.79, 153.77 (Ar*C*), [(152.33, d, $^{2}J_{C\text{-}P} = 6$ Hz, isomer A), (152.17, d, $^{2}J_{C\text{-}P} = 5.5$ Hz, isomer B) Ar*C*], 151.35, 151.31 (Ar*C*), 150.13 (*C*═O 2-nuc), 135.18, 134.99 (Ar*C*H), 132.64, 132.64 (*C*-3′), 127.20, 127.08 (*C*-2′), 125.37, 125.32 (Ar*C*H), 116.78 (Ar*C*), [(116.14, d, $^{3}J_{C\text{-}P} = 4.8$ Hz, isomer A), (115.96, d, $^{3}J_{C\text{-}P} = 5.4$ Hz, isomer B) Ar*C*H], 113.79, 113.73

(ArCH), 110.83, 110.68 (ArC), [(108.27, d, $^3J_{C\text{-}P}$ = 4.8 Hz, isomer A), (108.08, d, $^3J_{C\text{-}P}$ = 5.6 Hz, isomer B) ArCH], 89.43, 89.14 (C-1′), 84.00, 84.93 (C-4′), [(66.96, d, $^2J_{C\text{-}P}$ = 5.4 Hz, isomer A), (66.35, d, $^2J_{C\text{-}P}$ = 4.5 Hz, isomer B) C-5'], 61.36, 61.33 (CH_2 ester), 49.76, 49.67 (CH ala), 20.47-20.35 (m, CH_3 coum), 18.16 (CH_3 ala), 13.55 (CH_3 ester), 11.84, 11.80 (CH_3 nuc). MS [ESI, *m/z*]: 584.2 [M+Na]. MS [ESI, *m/z*]: HRMS calcd for $C_{25}H_{28}N_3O_{10}P$ [M+H], 562.1585; found, 562.1570.

4.1.7. Isopropyl (((5-(5-methyl-2,4-dioxo-3,4-dihydropyrimidin-1(2H)-yl)-2,5-dihydrofuran-2-yl)methoxy) ((4-methyl-2-oxo-2H-chromen-7-yl) oxy)phosphoryl)alaninate (20, pale yellow solid, yield 12 %)

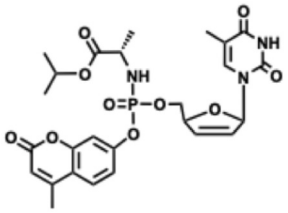

^{1}H NMR ($CDCl_3$, 500 MHz): δ 8.54, 8.50 (2bs, 1H, NH), 7.58 (dd, *J* = 8.5, 3 Hz, 1H, ArH), 7.31-7.17 (m, 3H, ArH), 7.07-7.02 (2 m, 1H, H-1′), [(6.40, dt, *J* = 6, 2 Hz, isomer A), (6.35, dt, *J* = 6, 2 Hz, isomer B), 1H, H-3'], 6.27 (m, 1H, ArH), 6.00-5.93 (m, 1H, H-2′), 5.11- 4.99 (m, 2H, H-4′, CH ester), 4.46-4.28 (m, 2H, H-5′), 4.04-3.84 (m, 2H, NH, CH ala), 2.44 (d, *J* = 1 Hz, 3H, CH_3 coum), 1.88, 1.84 (2d, *J* = 1.5, 1 Hz, 3H, CH_3 nuc), 1.40, 1.38 (2d, *J* = 7 Hz, 3H, CH_3 ala), 1.28-1.24 (m, 6H, 2CH_3 ester). ^{31}P NMR ($CDCl_3$, 202 MHz): δ 3.15, 2.57. ^{13}C NMR ($CDCl_3$, 125 MHz): δ [(172.87, d, $^3J_{C\text{-}P}$ = 7.5 Hz, isomer A), [(172.77, d, $^3J_{C\text{-}P}$ = 8.1 Hz, isomer B), C═O ester], 163.50, 163.48 (C═O 4-nuc), 160.39, 160.35 (C═O coum), 154.36, 154.34 (ArC), [(152.91, d, $^2J_{C\text{-}P}$ = 5.6 Hz, isomer A), (152.75, d, $^2J_{C\text{-}P}$ = 5.5 Hz, isomer B) ArC], 151.87, 151.83 (ArC), 150.66 (C═O 2-nuc), 135.72, 135.54 (ArCH), 133.15, 132.88 (C-3′), 127.75, 127.64 (C-2′), 125.90, 125.85 (ArCH), 117.31, 117.25 (ArC), 116.68, 116.53 (2d, $^3J_{C\text{-}P}$ = 5.1, 4.9 Hz, ArCH), 114.33, 114.28 (ArCH), 111.38, 111.22 (ArC), [(108.82, d, $^3J_{C\text{-}P}$ = 5.4 Hz, isomer A), (108.66, d, $^3J_{C\text{-}P}$ = 5.6 Hz, isomer B) ArCH], 89.96, 89.69 (C-1′), 84.54, 84.48 (2d, $^3J_{C\text{-}P}$ = 4.3 Hz,C-4′), 69.73, 69.69 (CH ester), [(67.44, d, $^2J_{C\text{-}P}$ = 5.5 Hz, isomer A), (66.89, d, $^2J_{C\text{-}P}$ = 4.6 Hz, isomer B) C-5'], 50.39, 50.29 (CH ala), 21.69, 21.61 ($(CH_3)_2$ ester), [(21.03, d, $^3J_{C\text{-}P}$ = 4.5 Hz, isomer A), (20.94, d, $^3J_{C\text{-}P}$ = 4.9 Hz, isomer B), CH_3 ala], 18.71 (CH_3 coum), 12.40, 12.36 (CH_3 nuc). MS [ESI, *m/z*]: 598.2, HRMS calcd for $C_{26}H_{30}N_3O_{10}P$ [M+H], 576.1742; found, 576.1734.

4.1.8. Benzyl (((5-(5-methyl-2,4-dioxo-3,4-dihydropyrimidin-1(2H)-yl)-2,5-dihydrofuran-2-yl)methoxy)((4-methyl-2-oxo-2H-chromen-7-yl)oxy) phosphoryl)alaninate (21, pale yellow solid, yield 15 %)

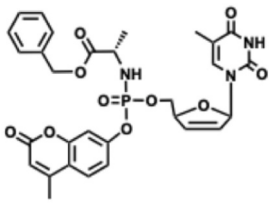

^{1}H NMR ($CDCl_3$, 500 MHz): δ 8.59 (bs, 1H, NH), 7.55, 7.53 (2d, *J* = 8.5 Hz, 1H, ArH), 7.41-7.31 (m, 5H, ArH), 7.28-7.11 (m, 3H, ArH), 7.04-6.98 (2 m, 1H, H-1′), 6.38-6.24 [(6.36, dt, *J* = 6, 2 Hz, isomer A), m, 2H, H-3′, ArH), 5.93 (d, *J* = 6 Hz, 1H, H-2′), 5.22- 5.12 (m, 2H, CH_2 ester), 5.05- 4.97 (2 m, 1H, H-4′), 4.40-4.22 (m, 2H, H-5′), 4.11-3.90 (m, 2H, NH, CH ala), 2.44-2.42 (m, 3H, CH_3 coum), 1.85, 1.80 (2d, *J* = 1 Hz, 3H, CH_3 nuc), 1.42, 1.40 (2d, *J* = 7 Hz, 3H, CH_3 ala). ^{31}P NMR ($CDCl_3$, 202 MHz): δ 2.99, 2.38. ^{13}C NMR ($CDCl_3$, 125 MHz): δ [(173.17, d, $^3J_{C\text{-}P}$ = 7.1 Hz, isomer A), [(173.03, d, $^3J_{C\text{-}P}$ = 7.8 Hz, isomer B), C═O ester], 163.45, 163.41 (C═O 4-nuc), 160.38, 160.34 (C═O coum), 154.34, 154.31 (ArC), [(152.83, d, $^2J_{C\text{-}P}$ = 6.4 Hz, isomer A), (152.68, d, $^2J_{C\text{-}P}$ = 5.9 Hz, isomer B) ArC], 151.86, 151.81 (ArC), 150.61, 150.59 (C═O 2-nuc), 135.68, 135.50 (ArCH), 135.07, 135.01 (*ipso* ArC), 133.16, 132.80 (C-3′), 128.70 (ArCH), 128.67 (ArCH), 128.30 (ArCH), 127.70, 127.58 (C-2′), 125.90, 125.83 (ArCH), 117.31, 117.27 (ArC), 116.65, 116.50 (2d, $^3J_{C\text{-}P}$ = 4.9, 4.8 Hz, ArCH), 114.34, 114.30 (ArCH), 111.33, 111.22 (ArC), [(108.82, d, $^3J_{C\text{-}P}$ = 5.1 Hz, isomer A), (108.66, d, $^3J_{C\text{-}P}$ = 5.5 Hz, isomer B) ArCH], 89.96, 89.69 (C-1′), 84.50, 84.44 (2d, $^3J_{C\text{-}P}$ = 6.5 Hz,C-4′), [(67.51, d, $^2J_{C\text{-}P}$ = 4.5 Hz, isomer A), (66.43, d, $^2J_{C\text{-}P}$ = 5.3 Hz, isomer B) C-5'], 66.91, 66.87 (CH_2 ester), 50.40, 50.27 (2d, $^2J_{C\text{-}P}$ = 1.6, 1.5 Hz, CH ala), [(20.95, d, $^3J_{C\text{-}P}$ = 4.8 Hz, isomer A), (20.85, d, $^3J_{C\text{-}P}$ = 5.6 Hz, isomer B), CH_3 ala], 18.71 (CH_3 coum), 12.40, 12.35 (CH_3 nuc). MS [ESI, *m/z*]: 646.2 [M+Na]. HRMS calcd for $C_{30}H_{30}N_3O_{10}P$ [M+H], 624.1742; found, 624.1737.

4.1.9. Methyl (((5-(5-methyl-2,4-dioxo-3,4-dihydropyrimidin-1(2H)-yl)-2,5-dihydrofuran-2-yl)methoxy) ((2-oxo-4-(trifluoromethyl)-2H-chromen-7-yl)oxy)phosphoryl)alaninate, (22, pale yellow solid, yield 7 %)

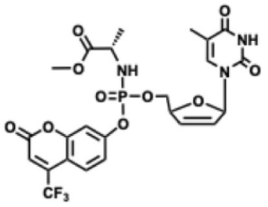

^{1}H NMR ($CDCl_3$, 500 MHz): δ 8.66, 8.62 (2s, 1H, NH), 7.72 (d, *J* = 9 Hz, 1H, ArH), 7.31 (ddd, *J* = 1, 2.5, 8 Hz, 1H, ArH), 7.28-7.26 (m, 1H, ArH), [(7.23, ddd, *J* = 1, 2.5, 9 Hz, isomer A), (7.21, q, *J* = 1.5 Hz, isomer B), 1H, ArH], 7.07-7.02 (2 m, 1H, H-1′), 6.78 (s, 1H, ArH), 6.41, 6.35 (2 dt, *J* = 2, 6 Hz, 1H, H-3′), 6.00-5.95 (m, 1H, H-2′), 5.11-5.05 (2 m, 1H, H-4′), 4.43-4.28 (m, 2H, H-5′), 4.10-3.92 (m, 2H, NH, CH ala), 3.77, 3.75 (2s, 3H, CH_3 ester), 1.89, 1.84 (2d, *J* = 1 Hz, 3H, CH_3 nuc), 1.43, 1.41 (2d, *J* = 7.5 Hz, 3H, CH_3 ala). ^{31}P NMR ($CDCl_3$, 202 MHz): δ 3.01, 2.42. ^{13}C NMR ($CDCl_3$, 125 MHz): δ 173.23 (C═O ester), 162.89 (C═O 4-nuc), 157.87 (C═O coum), 154.75 (ArC), 153.40 (ArC), 150.08 (C═O 2-nuc), 140.51 (q, $^2J_{C\text{-}F}$ = 31.3 Hz, ArC), 135.02, 134.86 (ArCH), 132.53, 132.16 (C-3′), 127.27, 127.14 (C-2′), 126.20 (ArCH), 120.80 (q, $^1J_{C\text{-}F}$ = 275.3 Hz, CF_3), 117.09, 116.91 (2d, $^3J_{C\text{-}P}$ = 2.5 Hz, ArCH), 114.67-114.40 (m, ArCH), 110.86, 110.71 (ArC), 110.12 (m, ArC), [(108.88, d, $^3J_{C\text{-}P}$ = 0.3 Hz, isomer A), (108.69, d,$^3J_{C\text{-}P}$ = 0.4 Hz, isomer B) ArCH], 89.49, 89.18 (C-1′), 83.88 (2d, $^3J_{C\text{-}P}$ = 4.5 Hz, C- 4′), [(67.15, d, $^2J_{C\text{-}P}$ = 5.4 Hz, isomer A), (66.46, d, $^2J_{C\text{-}P}$ = 4.5 Hz, isomer B) C-5'], 52.23 (CH_3 ester), 49.66, 49.60 (CH ala), 20.37 (2d, $^3J_{C\text{-}P}$ = 5 Hz, CH_3 ala), 11.86, 11.81 (CH_3 Nuc). ^{19}F NMR ($CDCl_3$, 470 MHz): δ −64.74. MS [ESI, *m/z*]: 624.10 [M+Na]. MS [ESI, *m/z*]: HRMS calcd for $C_{24}H_{23}F_3N_3O_{10}P$ [M+H], 602.1146; found, 602.1140.

4.1.10. Ethyl (((5-(5-methyl-2,4-dioxo-3,4-dihydropyrimidin-1(2H)-yl)-2,5-dihydrofuran-2- yl)methoxy)((2-oxo-4-(trifluoromethyl)-2H-chromen-7-yl)oxy)phosphoryl)alaninate (23, pale yellow solid, yield 11 %)

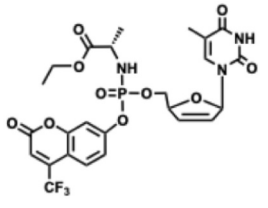

^{1}H NMR ($CDCl_3$, 500 MHz): δ 8.82, 8.78 (2s, 1H, NH), 7.71 (d, *J* = 9 Hz, 1H, ArH), 7.31 (s, 1H, ArH), 7.26-7.21 (m, 1H, ArH), 7.07-7.02 (2 m,

1H, *H*-1′), 6.78 (s, 1H, Ar*H*), [(6.40, d, $J = 5.5$ Hz, isomer A), (6.35, d, $J = 6$ Hz, isomer B), 1H, *H*-3'], 6.00-5.94 (m, 1H, *H*-2′), 5.11- 5.05 (m, 1H, *H*-4′), 4.44-4.29 (m, 2H, *H*-5′), 4.25-4.15 (m, 2H, CH_2 ester), 4.08-3.97 (m, 2H, N*H*, C*H* ala), 1.89, 1.84 (2s, 3H, CH_3 nuc), 1.41, 1.38 (2d, $J = 7.5$ Hz, 3H, CH_3 ala), 1.28 (t, $J = 7.5$ Hz, 3H, CH_3 ester). ^{31}P NMR ($CDCl_3$, 202 MHz): δ 3.11, 2.53. ^{19}F NMR ($CDCl_3$, 470 MHz): δ - 64.78. ^{13}C NMR ($CDCl_3$, 125 MHz): δ 172.79, 172.74 (*C*═O ester), 162.99 (*C*═O 4-nuc), 157.88, 157.82 (*C*═O coum), 154.71, 154.68 (Ar*C*), [(153.35, d, $^2J_{C\text{-}P} = 6.3$ Hz, isomer A), (153.18, d, $^2J_{C\text{-}P} = 5.4$ Hz, isomer B) Ar*C*], 150.12 (*C*═O 2-nuc), 140.43 (q, $^2J_{C\text{-}F} = 33.1$ Hz, Ar*C*), 135.07, 134.91 (Ar*C*H), 132.49, 132.18 (*C*-3′), 127.26, 127.16 (*C*-2′), 126.15 (Ar*C*H), 120.73 (q, $^1J_{C\text{-}F} = 273.8$ Hz, *C*F$_3$), 117.08, 116.89 (2d, $^3J_{C\text{-}P} = 5.2$ Hz, Ar*C*H), 114.62-114.40 (m, Ar*C*H), 110.84, 110.68 (Ar*C*), 110.17, 110.09 (Ar*C*), [(108.83, d, $^3J_{C\text{-}P} = 5.2$ Hz, isomer A), (108.64, d, $^3J_{C\text{-}P} = 5.5$ Hz, isomer B) Ar*C*H], 89.45, 89.15 (*C*-1′), 83.90, 83.83 (*C*-4′), [(67.09, d, $^2J_{C\text{-}P} = 5.5$ Hz, isomer A), (66.45, d, $^2J_{C\text{-}P} = 4.8$ Hz, isomer B) *C*-5'], 61.38 (*C*H$_2$ ester), 49.73, 49.65 (*C*H ala), [(20.40, d, $^3J_{C\text{-}P} = 4.6$ Hz, isomer A), (20.31, d, $^3J_{C\text{-}P} = 5.1$ Hz, isomer B), *C*H$_3$ ala], 13.51 (*C*H$_3$ ester), 11.84, 11.80 (*C*H$_3$ nuc). MS [ESI, *m/z*]: 638.2 [M+Na]. MS [ESI, *m/z*]: HRMS calcd for $C_{25}H_{25}F_3N_3O_{10}P$ [M+H], 616.1298; found, 616.1298.

4.1.11. Isopropyl (((5-(5-methyl-2,4-dioxo-3,4-dihydropyrimidin-1(2H)-yl)-2,5-dihydrofuran-2-yl)methoxy) ((2-oxo-4-(trifluoromethyl)-2H-chromen-7-yl)oxy)phosphoryl)alaninate, (24, pale yellow solid, yield 14 %)

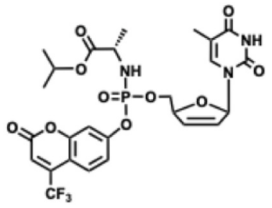

^{1}H NMR ($CDCl_3$, 500 MHz): δ 9.22 (bs, 1H, N*H*), 7.70 (d, $J = 9$ Hz, 1H, Ar*H*), 7.33-7.30 (m, 1H, Ar*H*), 7.29-7.27 (m, 1H, Ar*H*), 7.26-7.21 (m, 1H, Ar*H*),7.06-7.01 (m, 1H, *H*-1′), 6.76 (s, 1H, Ar*H*), [(6.40, dt, $J = 6$, 2 Hz, isomer A), (6.35, dt, $J = 6$, 2 Hz, isomer B), 1H, *H*-3'], 5.99-5.93 (m, 1H, *H*-2′), 5.11- 4.98 (m, 2H, *H*-4′, C*H* ester), 4.46-4.29 (m, 2H, *H*-5′), 4.28-4.18 (m, 1H, N*H*), 4.03-3.91 (m, 1H, C*H* ala), 1.87, 1.843 (2d, $J = 1$ Hz, 3H, CH_3 nuc), 1.39, 1.38 (2d, $J = 7.5$ Hz, 3H, CH_3 ala), 1.27-1.21 (m, 6H, 2CH_3 ester). ^{31}P NMR ($CDCl_3$, 202 MHz): δ 3.22, 2.66. ^{19}F NMR ($CDCl_3$, 470 MHz): δ - 64.80. ^{13}C NMR ($CDCl_3$, 125 MHz): δ [(172.90, d, $^3J_{C\text{-}P} = 7.1$ Hz, isomer A), [(172.75, d, $^3J_{C\text{-}P} = 8.1$ Hz, isomer B), *C*═O ester], 163.80 (*C*═O 4-nuc), 158.45, 158.41 (*C*═O coum), 155.26, 155.24 (Ar*C*), [(153.93, d, $^2J_{C\text{-}P} = 5.8$ Hz, isomer A), (153.76, d, $^2J_{C\text{-}P} = 5.9$ Hz, isomer B) Ar*C*], 150.84 (*C*═O 2-nuc), 141.01, 140.97 (2q, $^2J_{C\text{-}F} = 33$, 32.8 Hz, Ar*C*), 135.70, 135.56 (Ar*C*H), 133.03, 132.78 (*C*-3′), 127.81, 127.73 (*C*-2′), 126.70, 126.41 (Ar*C*H), 121.33 (q, $^1J_{C\text{-}F} = 273.9$ Hz, *C*F$_3$), 117.65, 116.48 (2d, $^3J_{C\text{-}P} = 5.4$, 5.3 Hz, Ar*C*H), 115.17, 114.96 (Ar*C*H), 111.40, 111.24 (2d, $^3J_{C\text{-}P} = 5.4$, 5.3 Hz, Ar*C*), 110.71, 110.64 ((Ar*C*), [(109.41, d, $^3J_{C\text{-}P} = 5.4$ Hz, isomer A), (109.24, d, $^3J_{C\text{-}P} = 5.5$ Hz, isomer B) Ar*C*H], 90.00, 89.73 (*C*-1′), 84.49, 84.42 (*C*-4′), 69.79, 69.75 (*C*H ester), [(67.65, d, $^2J_{C\text{-}P} = 5.4$ Hz, isomer A), (67.08, d, $^2J_{C\text{-}P} = 4.6$ Hz, isomer B), *C*-5'], 50.42, 50.32 (*C*H ala), 21.64, 21.57, (*C*H$_3$)$_2$ ester, [(20.94, d, $^3J_{C\text{-}P} = 4.4$ Hz, isomer A), (20.84, d, $^3J_{C\text{-}P} = 5.3$ Hz, isomer B), *C*H$_3$ ala], 12.40, 12.36 (*C*H$_3$ nuc). MS [ESI, *m/z*]: HRMS calcd for $C_{26}H_{27}F_3N_3O_{10}P$ [M+H], 630.1459; found, 630.1454.

4.1.12. Benzyl (((5-(5-methyl-2,4-dioxo-3,4-dihydropyrimidin-1(2H)-yl)-2,5-dihydrofuran-2-yl)methoxy)((2-oxo-4-(trifluoromethyl)-2H-chromen-7-yl)oxy)phosphoryl)alaninate (25, pale yellow solid, yield 12 %)

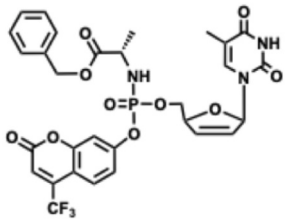

^{1}H NMR ($CDCl_3$, 500 MHz): δ 8.71, 8.67 (2bs, 1H, N*H*), 7.68, 7.67 (2d, $J = 8$, 8.5 Hz, 1H, Ar*H*), 7.41-7.31 (m, 5H, Ar*H*), 7.30-7.15 (m, 3H, Ar*H*), 7.05-6.99 (2 m, 1H, *H*-1′), 6.76 (s, 1H, Ar*H*), 6.36, 6.27 [2d, $J = 6$, 6.5 Hz, 1H, *H*-3′), 5.93 (d, $J = 6.5$ Hz 1H, *H*-2′), 5.20- 5.12 (m, 2H, CH_2 ester), 5.06- 4.98 (2 m, 1H, *H*-4′), 4.40-4.22 (m, 2H, *H*-5′), 4.11-3.99 (m, 2H, N*H*, C*H* ala), 1.86, 1.81 (2d, $J = 1$, 0.5 Hz, 3H, CH_3 nuc), 1.42, 1.41 (2d, $J = 6$. 6.5 Hz, 3H, CH_3 ala). ^{31}P NMR ($CDCl_3$, 202 MHz): δ 2.81, 2.34. ^{19}F NMR ($CDCl_3$, 470 MHz): δ - 64.78. ^{13}C NMR ($CDCl_3$, 125 MHz): δ [(173.09, d, $^3J_{C\text{-}P} = 6.4$ Hz, isomer A), [(172.92, d, $^3J_{C\text{-}P} = 7.3$ Hz, isomer B), *C*═O ester], 163.44, 163.43 (*C*═O 4-nuc), 158.41, 158.37 (*C*═O coum), 155.27, 155.23 (Ar*C*), [(153.88, d, $^2J_{C\text{-}P} = 6$ Hz, isomer A), (153.71, d, $^2J_{C\text{-}P} = 5.9$ Hz, isomer B) Ar*C*], 150.63, 150.61 (*C*═O 2-nuc), 141.00, 140.97 (2q, $^2J_{C\text{-}F} = 33.0$, 33.1 Hz, Ar*C*), 135.59, 135.43 (Ar*C*H), 135.01, 134.96 (*ipso* Ar*C*), 133.04, 132.70 (*C*-3′), 128.70, 128.68 (Ar*C*H), 128.63 (Ar*C*H), 128.30, 128.28 (Ar*C*H), 127.78, 127.67 (*C*-2′), 126.72, 126.69 (Ar*C*H), 121.34 (q, $^1J_{C\text{-}F} = 273.9$ Hz, *C*F$_3$), 117.57, 117.43 (2d, $^3J_{C\text{-}P} = 5.5$, 5.1 Hz, Ar*C*H), 115.10 (m, Ar*C*H), 111.36, 111.25 (Ar*C*), 110.71, 110.66 (Ar*C*), [(109.39, d, $^3J_{C\text{-}P} = 5.3$ Hz, isomer A), (109.22, d, $^3J_{C\text{-}P} = 5.8$ Hz, isomer B) Ar*C*H], 90.01, 89.73 (*C*-1′), 84.45, 84.37 (2d, $^3J_{C\text{-}P} = 3.4$, 3.3 Hz, *C*-4′), [(67.63, d, $^2J_{C\text{-}P} = 5.3$ Hz, isomer A), (67.55, d, $^2J_{C\text{-}P} = 2.8$ Hz, isomer B) *C*-5'], 67.07, 67.03 (*C*H$_2$ ester), 50.40, 50.29 (*C*H ala), [(20.90, d, $^3J_{C\text{-}P} = 4.8$ Hz, isomer A), (20.81, d, $^3J_{C\text{-}P} = 5.4$ Hz, isomer B), *C*H$_3$ ala], 12.42, 12.38 (*C*H$_3$ nuc). MS [ESI, *m/z*]: HRMS calcd for $C_{30}H_{27}F_3N_3O_{10}P$ [M + NH_4], 695.1724; found, 695.1721.

4.1.13. Ethyl (((1-ethoxy-1-oxopropan-2-yl)amino)((5-(5-methyl-2,4-dioxo-3,4-dihydropyrimidin-1(2H)-yl)-2,5-dihydrofuran-2-yl)methoxy) phosphoryl)alaninate (26, pale yellow solid, yield 4 %)

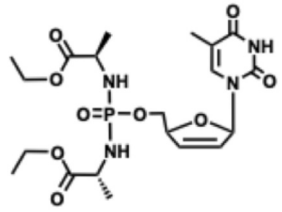

^{1}H NMR ($CDCl_3$, 500 MHz): δ 8.29 (s, 1H, N*H*), 7.30 (q, $J = 1$ Hz, 1H, Ar*H*), 7.05-7.03 (m, 1H, *H*-1′), 6.37, 6.35 (dt, $J = 1.5$, 6 Hz, 1H, *H*-3′), 5.92-5.89 (2 m, 1H, *H*-2′), 5.04-5.00 (m, 1H, *H*-4′), 4.26-4.15 (m, 6H, CH_2 ester, *H*-5′), 3.99-3.90 (m, 2H, C*H* ala), 3.39, 3.33 (2t, $J = 9.5$Hz,2H, N*H*ala),1.95 (d, $J = 1$Hz, 3H, CH_3 nuc), 1.40 (d, $J = 7$ Hz, 6H, CH_3 ala), 1.29 (t, $J = 7$ Hz, 6H, CH_3 ester). ^{31}P NMR ($CDCl_3$, 202 MHz): δ 12.18.

^{13}C NMR ($CDCl_3$, 125 MHz): δ 173.39, 173.34 (*C*═O ester), 162.81 (*C*═O 4-nuc), 149.99 (*C*═O 2-nuc), 135.08 (Ar*C*H), 132.90 (*C*-3′), 126.53 (*C*-2′), 110.77 (Ar*C*), 89.12 (*C*-1′), 84.34 (d, $^3J_{c\text{-}p}$ = 8 Hz, *C*-4′), 65.32 (d, $^2J_{C\text{-}P}$ = 5.3 Hz, *C*-5'), 60.91 (d, $^5J_{C\text{-}P}$ = 2.3 Hz, *C*H$_2$ ester), 49.27 (*C*H ala A), 48.95 (d, $^2J_{c\text{-}p}$ = 2.1 Hz, *C*H ala B), 20.42 (2d, $^3J_{c\text{-}p}$ = 5.5 Hz, *C*H$_3$ ala), 13.49 (*C*H$_3$ ester), 11.75 (*C*H$_3$ nuc). MS [ESI, *m/z*]: 525.2 [M+Na]. MS [ESI, *m/z*]: HRMS calcd for $C_{20}H_{31}N_4O_9P$ [M+H], 503.1901; found, 503.1899.

4.1.14. Benzyl (((1-benzoxy-1-oxopropan-2-yl)amino)((5-(5-methyl-2,4-dioxo-3,4-dihydro pyrimidin-1(2H)-yl)-2,5-dihydrofuran-2-yl)methoxy) phosphoryl)alaninate (27, pale yellow solid, yield 2 %)

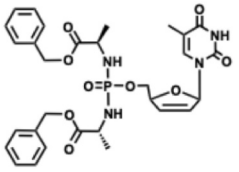

^{1}H NMR ($CDCl_3$, 500 MHz): δ 8.21 (s, 1H, N*H*), 7.41-7.32 (m, 10H, Ar*H*), 7.26 (q, *J* = 1 Hz, 1H, Ar*H*), 7.02-7.00 (m, 1H, *H*-1′), 6.27, 6.26 (dt, *J* = 1.5, 6 Hz, 1H, *H*-3′), 5.86 (ddd, *J* = 1, 1.5, 3.5 Hz, 1H, *H*-2′), 5.21-5.10 (m, 4H, C*H*$_2$ ester), 4.95-4.91 (m, 1H, *H*-4′), 4.18-4.09 (m, 2H, *H*-5′), 4.04-3.95 (m, 2H, C*H* ala), 3.36, 3.31 (2t, *J* = 10 Hz, 2H, N*H* ala), 1.93 (d, *J* = 1 Hz, 3H, C*H*$_3$ nuc), 1.39, 1.36 (2d, *J* = 7 Hz, 6H, C*H*$_3$ ala). ^{31}P NMR ($CDCl_3$, 202 MHz): δ 11.91. ^{13}C NMR ($CDCl_3$, 125 MHz): δ 173.85 (2d, $^3J_{C\text{-}P}$ = 2.8 Hz, *C*═O ester), 163.46 (*C*═O 4-nuc), 150.62 (*C*═O 2-nuc), 135.71 (Ar*C*), 135.33 (Ar*C*H), 135.26 (*C*-3′), 128.68, 128.65 (Ar*C*H), 128.56, 128.51 (Ar*C*H), 128.27 (Ar*C*H), 127.09 (*C*-2′), 111.41 (Ar*C*), 89.79 (*C*-1′), 84.94 (d, $^3J_{C\text{-}P}$ = 7.5 Hz, *C*-4′), 67.25 (d, $^2J_{C\text{-}P}$ = 6.6 Hz, *C*-5'), 66.08, 66.04 (CH$_2$ ester), 49.98, 49.73 (*C*H ala), 20.89 (t, $^2J_{C\text{-}P}$ = 5.5 Hz, *C*H$_3$ ala), 12.40, 11.80 (*C*H$_3$ nuc). MS [ESI, *m/z*]: 649.2 [M+Na]. MS [ESI, *m/z*]: HRMS calcd for $C_{30}H_{35}N_4O_9P$ [M + NH_4], 644.2480; found, 644.2476.

4.1.15. Ethyl (((1-ethoxy-1-oxopropan-2-yl)amino)((2-oxo-4-(trifluoromethyl)-2H-chromen-7-yl)oxy)phosphoryl)alaninate (28, pale yellow solid, yield 4 %)

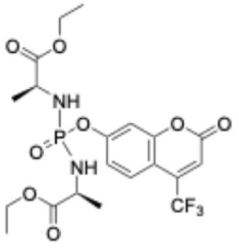

^{1}H NMR ($CDCl_3$, 500 MHz): δ 7.65 (d, *J* = 7.5 Hz, 1H, Ar*H*), 7.48 (dd, *J* = 9, 2 Hz, 1H, Ar*H*), 7.30 (m, 1H, Ar*H*), 7.25 (d, *J* = 8.5, 2 Hz, 1H, Ar*H*), 4.20 (m, 4H, 2C*H*$_2$), 4.07 (m, 2H, 2C*H*), 3.98 (m, 2H, 2N*H*), 1.45 (d, *J* = 7.5 Hz, 6H, 2C*H*$_3$), 1.27 (dt, *J* = 7, 1.5 Hz, 6H, 2C*H*$_3$). ^{19}F NMR ($CDCl_3$, 470 MHz): δ - 64.87. ^{31}P NMR ($CDCl_3$, 202 MHz): δ 8.31. ^{13}C NMR ($CDCl_3$, 125 MHz): δ 173.72 (2d, $^3J_{C\text{-}P}$ = 6.3 Hz, *C*═O ester), 162.10 (*C*═O), 159.87 (Ar*C*), 158.60 (Ar*C*), 141.42 (q, $^2J_{C\text{-}F}$ = 32.5 Hz, Ar*C*), 126.49 (Ar*C*H), 121.33 (q, $^1J_{C\text{-}F}$ = 273.5 Hz, *C*F$_3$), 117.82 (d, $^3J_{C\text{-}P}$ = 5.0 Hz, Ar*C*H), 114.68 (q, $^3J_{C\text{-}F}$ = 5.8 Hz, Ar*C*H), 110.28 (Ar*C*), 109.48 (d, $^3J_{C\text{-}P}$ = 5.4 Hz, Ar*C*H), 61.77 (*C*H$_2$), 50.15, 49.99 (*C*H), 20.83 (2d, $^3J_{C\text{-}P}$ = 4.3 Hz), *C*H$_3$ ala, 14.04 (*C*H$_3$). MS [ESI, *m/z*]: 509.2 [M+H]. MS [ESI, *m/z*]: HRMS calcd for $C_{20}H_{24}F_3N_2O_8P$ [M+H], 509.1295; found, 509.1282.

4.1.16. Benzyl (((1-benzoxy-1-oxopropan-2-yl)amino)((2-oxo-4-(trifluoromethyl)-2H-chromen-7-yl)oxy)phosphoryl)alaninate, (29, pale yellow solid, yield 3 %)

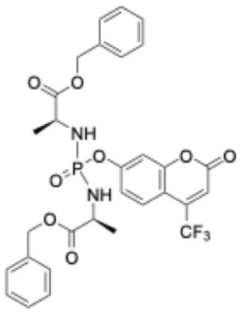

^{1}H NMR ($CDCl_3$, 500 MHz): δ 7.54 (d, *J* = 7.5 Hz, 1H, Ar*H*), 7.18 (m, 10H, Ar*H*), 7.18 (d, *J* = 9 Hz, 1H, Ar*H*), 7.10 (d, *J* = 9 Hz, 1H, Ar*H*), 6.63 (s, 1H, Ar*H*), 5.02 (m, 4H, 2C*H*$_2$), 4.04 (m, 2H, 2C*H*), 3.63 (m, 2H, 2N*H*), 1.32 (dt, *J* = 7.5, 2 Hz, 6H, 2C*H*$_3$). ^{19}F NMR ($CDCl_3$, 470 MHz): δ - 64.77. ^{31}P NMR ($CDCl_3$, 202 MHz): δ 7.84. ^{13}C NMR ($CDCl_3$, 125 MHz): δ 173.60 (2d, $^3J_{C\text{-}P}$ = 6.3 Hz, *C*═O ester), 158.65 (*C*═O), 155.29 (Ar*C*), 154.58 (Ar*C*), 140.97 (q, $^2J_{C\text{-}F}$ = 31.3 Hz, Ar*C*), 135.21, 135.19 (Ar*C*), 128.67 (Ar*C*H), 128.54 (Ar*C*H), 128.23 (Ar*C*H), 126.46 (Ar*C*H), 121.41 (q, $^1J_{C\text{-}F}$ = 273.8 Hz, *C*F$_3$), 117.78 (d, $^3J_{C\text{-}P}$ = 5.0 Hz, Ar*C*H), 114.68 (Ar*C*H), 111.21 (Ar*C*), 109.35 (d, $^3J_{C\text{-}P}$ = 5.0 Hz, Ar*C*H), 67.36, 67.33 (*C*H$_2$), 50.17, 50.06 (*C*H), 20.88 (2d, $^3J_{C\text{-}P}$ = 6.3 Hz), *C*H$_3$ ala. MS [ESI, *m/z*]: 632.2 [M+H]. MS [ESI, *m/z*]: HRMS calcd for $C_{30}H_{28}F_3N_2O_8P$ [M+H], 633.1608; found, 633.1604.

4.2. Antiviral activity

Tetrazolium-based colorimetric (MTS) assay for the detection of anti-HIV compounds. **[**81, 82]

Anti-HIV assays: The anti-HIV activity and cytotoxicity of the compounds **17–27**, 4MU and 4TFMU were evaluated against wild-type HIV-1 strain III$_B$, HIV-2 strain in MT-4, C8166 and C8166 TK$^-$ cell cultures using the MTS method. Briefly, stock solutions (10 × final concentration) of test compounds were added in 25 μL volumes to two series of triplicate wells to allow simultaneous evaluation of their effects on mock-and HIV-infected cells at the beginning of each experiment. Serial 5-fold dilutions of test compounds were made directly in flat-bottomed 96-well microtiter trays using a Biomek 4000 robot (Beckman Coulter Inc.). Untreated control HIV-and mock-infected cell samples were included for each sample. Virus stock (50 μL) at 100–300 $CCID_{50}$ (50 % cell culture infectious dose) or culture medium was added to either the virus-infected or mock-infected wells of the microtiter tray. Mock-infected cells were used to evaluate the effect of test compounds on uninfected cells to assess the cytotoxicity of the test compounds. Exponentially growing MT-4 cells were centrifuged for 5 min at 220 g and the supernatant was discarded. The MT-4 cells were resuspended at 5 × 10^5 cells/mL and 50 μL volumes were transferred to the microtiter tray wells. Five days after infection, the viability of mock-and HIV-infected cells was examined spectrophotometrically using the MTS assay.

The MTS assay is based on the reduction of yellow coloured MTS salt (Promega: G1111) by mitochondrial dehydrogenase activity of metabolically active cells to a brown–purple formazan that can be measured spectrophotometrically. The absorbances were read in a computer-controlled SPARK Reader and Stacker (Tecan), at two wavelengths (490 and 690 nm). All data were calculated using the median OD (optical density) values of three wells. The 50 % cytotoxic concentration (CC_{50}) was defined as the concentration of the test compound that reduced the absorbance (OD_{490}) of the mock-infected control sample by 50 %. The concentration achieving 50 % protection from the cytopathic effect of the virus in infected cells was defined as the 50 % effective

concentration (EC_{50}).

CRediT authorship contribution statement

Sahar B. Kandil: Writing – review & editing, Writing – original draft, Visualization, Validation, Supervision, Methodology, Investigation, Funding acquisition, Formal analysis, Data curation, Conceptualization. **Katie S. Jones:** Writing – review & editing, Investigation. **Christophe Pannecouque:** Writing – review & editing, Validation, Resources, Investigation, Data curation. **Andrew D. Westwell:** Writing – review & editing, Validation, Supervision, Resources, Project administration, Funding acquisition.

Declaration of competing interest

The authors declare the following financial interests/personal relationships which may be considered as potential competing interests: Andrew A Westwell reports financial support was provided by Welsh Government (Life Sciences Research Network Wales). If there are other authors, they declare that they have no known competing financial interests or personal relationships that could have appeared to influence the work reported in this paper.

Acknowledgments

The authors gratefully acknowledge Life Sciences Research Network Wales (Welsh Government, Ser Cymru) for providing postdoctoral support to SK. We thank Mrs. Kristien Erven, Mr. Kris Uyttersprot and Mrs. Cindy Heens for the technical assistance with HIV experiments and David Noakes for his technical support in chemistry experiments. We also acknowledge the EPSRC National Mass Spectrometry centre (Swansea, UK) for provision of accurate mass spectrometry. This work is dedicated to the memory of Professor Chris McGuigan.

Appendix A. Supplementary data

Supplementary data to this article can be found online at https://doi.org/10.1016/j.ejmech.2025.118543.

List of Abbreviations used

AIDS	acquired immunodeficiency syndrome
ADMET	Absorption, Distribution, Metabolism, Excretion, and Toxicity
AUC	Area Under the Curve
BBB	Blood–Brain Barrier
CC_{50}	half-maximal Cytotoxic Concentration
cART	Combination Antiretroviral Therapy
d4T	Stavudine
Et_3N	Triethylamine
FDA	Food and Drug Administration
GI	Gastrointestinal
HBV	Hepatitis B Virus
HCMV	Human Cytomegalovirus
HCV	Hepatitis C Virus
HIV	Human Immunodeficiency Virus
HRMS	High-Resolution Mass Spectrometry
HSV	Herpes Simplex Virus
IC_{50}	half-maximal Inhibitory Concentration
MS	Mass Spectrometry
MTS	Tetrazolium-based colorimetric assay
NAMP	Nucleoside Analogue Monophosphate
NAs	Nucleoside Analogues
NATP	Nucleoside Analogue Triphosphate
NMR	Nuclear Magnetic Resonance (^{1}H, ^{13}C, ^{19}F, ^{31}P)
NRTI	Nucleoside reverse transcriptase inhibitor
OD	Optical Density
$POCl_3$	Phosphorus Oxychloride
ProTide	Prodrug nucleotide (5′-aryloxyphosphoramidate)
SAR	Structure–Activity Relationship
SI	Selectivity Index
THF	Tetrahydrofuran
TLC	Thin Layer Chromatography
TPSA	Topological Polar Surface Area
UV	Ultraviolet
4MU	4-Methylumbelliferone
4TFMU	4-trifluoromethylumbelliferone

Data availability

Data will be made available on request.

References

[1] UNAIDS, Global HIV & AIDS statistics fact sheet, UNAIDS. https://www.unaids.org/en/resources/fact-sheet, 2024. (Accessed 7 October 2025).
[2] J.C. Reed, D. Solas, A. Kitaygorodskyy, B. Freeman, D.T.B. Ressler, D.J. Phuong, J. V. Swain, K. Matlack, C.R. Hurt, V.R. Lingappa, J.R. Lingappa, Identification of an antiretroviral small molecule that appears to be a host-targeting inhibitor of HIV-1 assembly, J. Virol. 95 (2021), https://doi.org/10.1128/JVI.00883-20 e00883-20.
[3] L. Hruba, V. Das, M. Hajduch, P. Dzubak, Nucleoside-based anticancer drugs: mechanism of action and drug resistance, Biochem. Pharmacol. 215 (2023) 115741, https://doi.org/10.1016/j.bcp.2023.115741.
[4] Y. Zhang, C. Fan, J. Zhang, X. Tian, W. Zuo, K. He, Lipid-conjugated nucleoside monophosphate and monophosphonate prodrugs: a versatile drug delivery paradigm, Eur. J. Med. Chem. 275 (2024) 116614, https://doi.org/10.1016/j.ejmech.2024.116614.
[5] D.S. Siegel, H.C. Hui, J. Pitts, M.S. Vermillion, K. Ishida, D. Rautiola, M. Keeney, H. Irshad, L. Zhang, K. Chun, G. Chin, B. Goyal, E. Doerffler, H. Yang, M.O. Clarke, C. Palmiotti, A. Vijjapurapu, N.C. Riola, K. Stray, E. Murakami, B. Ma, T. Wang, X. Zhao, Y. Xu, G. Lee, B. Marchand, M. Seung, A. Nayak, A. Tomkinson, N. Kadrichu, S. Ellis, O. Barauskas, J.Y. Feng, J.K. Perry, M. Perron, J.P. Bilello, P. J. Kuehl, R. Subramanian, T. Cihlar, R.L. Mackman, Discovery of GS-7682, a novel 4'-cyano-modified C-nucleoside prodrug with broad activity against pneumo- and picornaviruses and efficacy in RSV-infected African green monkeys, J. Med. Chem. 67 (2024) 12945–12968, https://doi.org/10.1021/acs.jmedchem.4c00899.
[6] K.L. Seley-Radtke, M.K. Yates, The evolution of nucleoside analogue antivirals: a review for chemists and non-chemists. Part 1: early structural modifications to the nucleoside scaffold, Antivir. Res. 154 (2018) 66–86, https://doi.org/10.1016/j.antiviral.2018.04.004.
[7] C. McGuigan, R.N. Pathirana, J. Balzarini, E. De Clercq, Intracellular delivery of bioactive AZT nucleotides by aryl phosphate derivatives of AZT, J. Med. Chem. 36 (1993) 1048–1052, https://doi.org/10.1021/jm00059a007.
[8] A. Thiraporn, T. Tiyasakulchai, T. Khamkhenshorngphanuch, M. Hoarau, R. Thiabma, S. Onnome, A. Suphatrakul, J. Narkpuk, C. Srisaowakarn, S. Manopwisedjaroen, K. Srichomthong, S. Hongeng, A. Thitithanyanont, P. Jaru-Ampornpan, S. Theeramunkong, B. Siridechadilok, N. Srimongkolpithak, Synthesis and modification of cordycepin-phosphoramidate ProTide derivatives for antiviral activity and metabolic stability, ACS Bio. Med. Chem. Au. 5 (2024) 89–105, https://doi.org/10.1021/acsbiomedchemau.4c00071.
[9] L. Zhang, G. Jia, Z. Li, S. Sun, Y. Chen, J. Zhao, X. Wang, W. Xu, F. Jing, Y. Jiang, X. Li, Design, synthesis, and anti-cancer evaluation of the novel conjugate of gemcitabine's ProTide prodrug based on CD13, Bioorg. Chem. 157 (2025) 108293, https://doi.org/10.1016/j.bioorg.2025.108293.
[10] G. Pastuch-Gawołek, D. Gillner, E. Król, K. Walczak, I. Wandzik, Selected nucleos(t)ide-based prescribed drugs and their multi-target activity, Eur. J. Pharmacol. 865 (2019) 172747, https://doi.org/10.1016/j.ejphar.2019.172747.
[11] A.J. Wiemer, D.F. Wiemer, Prodrugs of phosphonates and phosphates: crossing the membrane barrier, Top. Curr. Chem. 360 (2015) 115–160, https://doi.org/10.1007/128_2014_561.
[12] M.J. Sofia, D. Bao, W. Chang, J. Du, D. Nagarathnam, S. Rachakonda, P.G. Reddy, B.S. Ross, P. Wang, H.R. Zhang, S. Bansal, C. Espiritu, M. Keilman, A.M. Lam, H. M. Steuer, C. Niu, M.J. Otto, P.A. Furman, Discovery of a β-d-2'-deoxy-2'-α-fluoro-2'-β-C-methyluridine nucleotide prodrug (PSI-7977) for the treatment of hepatitis C virus, J. Med. Chem. 53 (2010) 7202–7218, https://doi.org/10.1021/jm100863x.
[13] E. Murakami, T. Wang, Y. Park, J. Hao, E.I. Lepist, D. Babusis, A.S. Ray, Implications of efficient hepatic delivery by tenofovir alafenamide (GS-7340) for hepatitis B virus therapy, Antimicrob. Agents Chemother. 59 (2015) 3563–3569, https://doi.org/10.1128/AAC.00128-15.
[14] J. Li, S. Liu, J. Shi, H.J. Zhu, Activation of tenofovir alafenamide and sofosbuvir in the human lung and its implications in the development of nucleoside/nucleotide prodrugs for treating SARS-CoV-2 pulmonary infection, Pharmaceutics 13 (2021) 1656, https://doi.org/10.3390/pharmaceutics13101656.
[15] P. Spiliopoulou, F. Kazmi, F. Aroldi, T. Holmes, D. Thompson, L. Griffiths, C. Qi, M. Parkes, S. Lord, G.J. Veal, D.J. Harrison, V.M. Coyle, J. Graham, T.R.J. Evans, S. P. Blagden, A phase I open-label, dose-escalation study of NUC-3373, a targeted thymidylate synthase inhibitor, in patients with advanced cancer (NuTide:301),

J. Exp. Clin. Cancer Res. 43 (2024) 100, https://doi.org/10.1186/s13046-024-03010-1.
[16] S. Kandil, C. Pannecouque, F.M. Chapman, A.D. Westwell, C. McGuigan, Polyfluoroaromatic stavudine (d4T) ProTides exhibit enhanced anti-HIV activity, Bioorg. Med. Chem. Lett. 29 (2019) 126721, https://doi.org/10.1016/j.bmcl.2019.126721.
[17] J.H. Vernachio, B. Bleiman, K.D. Bryant, S. Chamberlain, D. Hunley, J. Hutchins, B. Ames, E. Gorovits, B. Ganguly, A. Hall, A. Kolykhalov, Y. Liu, J. Muhammad, N. Raja, C.R. Walters, J. Wang, K. Williams, J.M. Patti, G. Henson, K. Madela, M. Aljarah, A. Gilles, C. McGuigan, INX-08189, a phosphoramidate prodrug of 6-O-methyl-2'-C-methyl guanosine, is a potent inhibitor of hepatitis C virus replication with excellent pharmacokinetic and pharmacodynamic properties, Antimicrob. Agents Chemother. 55 (2011) 1843–1851, https://doi.org/10.1128/AAC.01335-10.
[18] S. Kandil, J. Balzarini, S. Rat, A. Brancale, A.D. Westwell, C. McGuigan, ProTides of BVdU as potential anticancer agents upon efficient intracellular delivery of their activated metabolites, Bioorg. Med. Chem. Lett. 26 (2016) 5618–5623, https://doi.org/10.1016/j.bmcl.2016.10.077.
[19] K.Y. Hostetler, L.M. Stuhmiller, H.B. Lenting, H. Van Den Bosch, D.D. Richman, Synthesis and antiretroviral activity of phospholipid analogs of azidothymidine and other antiviral nucleosides, J. Biol. Chem. 265 (1990) 6112–6117.
[20] C. Meier, 2-Nucleos-5'-O-yl-4H-1,2,3-benzodioxaphosphinin-2-oxides – a new concept for lipophilic, potential prodrugs of biologically active nucleoside monophosphates, Angew. Chem. Int. Ed. 35 (1996) 70–72.
[21] R.L. Mackman, Phosphoramidate prodrugs continue to deliver: the journey of remdesivir (GS-5734) from RSV to SARS-CoV-2, ACS Med. Chem. Lett. 13 (2022) 338–347, https://doi.org/10.1021/acsmedchemlett.1c00624.
[22] C. McGuigan, C. Bourdin, M. Derudas, N. Hamon, K. Hinsinger, S. Kandil, K. Madela, S. Meneghesso, F. Pertusati, M. Serpi, M. Slusarczyk, S. Chamberlain, A. Kolykhalov, J. Vernachio, C. Vanpouille, A. Introini, L. Margolis, J. Balzarini, Design, synthesis and biological evaluation of phosphorodiamidate prodrugs of antiviral and anticancer nucleosides, Eur. J. Med. Chem. 70 (2013) 326–340.
[23] C. McGuigan, K. Madela, M. Aljarah, C. Bourdin, M. Arrica, E. Barrett, S. Jones, A. Kolykhalov, B. Bleiman, K.D. Bryant, B. Ganguly, E. Gorovits, G. Henson, D. Hunley, J. Hutchins, J. Muhammad, A. Obikhod, J. Patti, C.R. Walters, J. Wang, J. Vernachio, C.V. Ramamurty, S.K. Battina, S. Chamberlain, Phosphorodiamidates as a promising new phosphate prodrug motif for antiviral drug discovery: application to anti-HCV agents, J. Med. Chem. 54 (2011) 8632–8645.
[24] N. Magula, M. Dedicoat, Low dose versus high dose stavudine for treating people with HIV infection, Cochrane Database Syst. Rev. 28 (2015) 1.
[25] F.M. Uckun, P. Cahn, D. Qazi, O. D'Cruz, Stampidine as a promising antiretroviral drug candidate for pre-exposure prophylaxis against sexually transmitted HIV/AIDS, Expet Opin. Invest. Drugs 21 (2012) 489–500.
[26] K. Sahin, C. Orhan, I.H. Ozercan, M. Tuzcu, B. Elibol, T.K. Sahin, U. Kilic, S. Qazi, F.M. Uckun, Chemopreventive efficacy of stampidine in a murine breast cancer model, Expert Opin. Ther. Targets 24 (2020) 155–162, https://doi.org/10.1080/14728222.2020.1724961.
[27] V. Flores-Morales, A.P. Villasana-Ruíz, I. Garza-Veloz, S. González-Delgado, M. L. Martinez-Fierro, Therapeutic effects of coumarins with different substitution patterns, Molecules 28 (2023) 2413, https://doi.org/10.3390/molecules28052413.
[28] F. Saadati, A. Modarresi Chahardehi, N. Jamshidi, N. Jamshidi, D. Ghasemi, Coumarin: a natural solution for alleviating inflammatory disorders, Curr. Res. Pharmacol. Drug Discov. 7 (2024) 100202, https://doi.org/10.1016/j.crphar.2024.100202.
[29] S. Kandil, A.D. Westwell, C. McGuigan, 7-Substituted umbelliferone derivatives as androgen receptor antagonists for the potential treatment of prostate and breast cancer, Bioorg. Med. Chem. Lett. 26 (2016) 2000–2004, https://doi.org/10.1016/j.bmcl.2016.02.088.
[30] M.Z. Hassan, H. Osman, M.A. Ali, M.J. Ahsan, Therapeutic potential of coumarins as antiviral agents, Eur. J. Med. Chem. 123 (2016) 236–255, https://doi.org/10.1016/j.ejmech.2016.07.056.
[31] S. Mishra, A. Pandey, S. Manvati, Coumarin: an emerging antiviral agent, Heliyon 6 (2020) e03217, https://doi.org/10.1016/j.heliyon.2020.e03217.
[32] M. Suleiman, F.A. Almalki, T. Ben Hadda, S.M.A. Kawsar, S. Chander, S. Murugesan, A.R. Bhat, A. Bogoyavlenskiy, J. Jamalis, Recent progress in synthesis, POM analyses and SAR of coumarin-hybrids as potential anti-HIV agents – a mini review, Pharmaceuticals 16 (2023) 1538, https://doi.org/10.3390/ph16111538.
[33] M. Mazzei, E. Nieddu, M. Miele, A. Balbi, M. Ferrone, M. Fermeglia, M.T. Mazzei, S. Pricl, P. La Colla, F. Marongiu, C. Ibba, R. Loddo, Activity of Mannich bases of 7-hydroxycoumarin against *Flaviviridae*, Bioorg. Med. Chem. 16 (2008) 2591–2605, https://doi.org/10.1016/j.bmc.2007.11.045.
[34] L. Pohjala, A. Utt, M. Varjak, A. Lulla, A. Merits, T. Ahola, P. Tammela, Inhibitors of alphavirus entry and replication identified with a stable Chikungunya replicon cell line and virus-based assays, PLoS One 6 (2011) e28923, https://doi.org/10.1371/journal.pone.0028923.
[35] Y. Kashman, K.R. Gustafson, R.W. Fuller, J.H. Cardellina II, J.B. McMahon, M. J. Currens, R.W. Buckheit Jr., S.H. Hughes, G.M. Cragg, M.R. Boyd, The calanolides, a novel HIV-inhibitory class of coumarin derivatives from the tropical rainforest tree, *Calophyllum lanigerum*, J. Med. Chem. 35 (1992) 2735–2743, https://doi.org/10.1021/jm00093a004.
[36] Z.Q. Xu, M.T. Flavin, T.R. Jenta, Calanolides, the naturally occurring anti-HIV agents, Curr. Opin. Drug Discov. Dev 3 (2000) 155–166.
[37] R.Z. Batran, A. Sabt, M.A. Khedr, A.K. Allayeh, C. Pannecouque, A.F. Kassem, 4-Phenylcoumarin derivatives as new HIV-1 NNRTIs: design, synthesis, biological activities, and computational studies, Bioorg. Chem. 141 (2023) 106918, https://doi.org/10.1016/j.bioorg.2023.106918.
[38] A.D. Sharapov, R.F. Fatykhov, I.A. Khalymbadzha, G.V. Zyryanov, O. N. Chupakhin, M.V. Tsurkan, Plant coumarins with anti-HIV activity: isolation and mechanisms of action, Int. J. Mol. Sci. 24 (2023) 2839.
[39] Z. Xu, Q. Chen, Y. Zhang, C. Liang, Coumarin-based derivatives with potential anti-HIV activity, Fitoterapia 150 (2021) 104863.
[40] A. Gupta, N. Singh, A. Gautam, N. Dhakar, S. Kumar, P.K. Sasmal, Visible and NIR light photoactivatable o-hydroxycinnamate system for efficient drug release with fluorescence monitoring, RSC Med. Chem. 14 (2023) 1088–1100, https://doi.org/10.1039/d2md00438k.
[41] D. Cao, Z. Liu, P. Verwilst, S. Koo, P. Jangili, J.S. Kim, W. Lin, Coumarin-based small-molecule fluorescent chemosensors, Chem. Rev. 119 (2019) 10403–10519, https://doi.org/10.1021/acs.chemrev.9b00145.
[42] A.M. Olowolagba, M.O. Idowu, D.L. Arachchige, O.R. Aworinde, S.K. Dwivedi, O. R. Graham, T. Werner, R.L. Luck, H. Liu, Syntheses and applications of coumarin-derived fluorescent probes for real-time monitoring of NAD(P)H dynamics in living cells across diverse chemical environments, ACS Appl. Bio Mater. 7 (2024) 5437–5451, https://doi.org/10.1021/acsabm.4c00595.
[43] S.M. Mantovani, L.G. Oliveira, A.J. Marsaioli, Esterase screening using whole cells of Brazilian soil microorganisms, J. Braz. Chem. Soc. 21 (2010) 1484–1489.
[44] A.A. Tsitrina, N. Halimani, I.N. Andreichenko, M. Sabirov, M. Nesterchuk, N. O. Dashenkova, R. Romanov, E.V. Bulgakova, A. Mikaelyan, Y. Kotelevtsev, 4-Methylumbelliferone targets revealed by public data analysis and liver transcriptome sequencing, Int. J. Mol. Sci. 24 (2023) 2129, https://doi.org/10.3390/ijms24032129.
[45] M. Samanth, M. Bhat, Synthesis and importance of coumarin derivatives in medicinal chemistry: a comprehensive review, Russ. J. Bioorg. Chem. 50 (2024) 1672–1691.
[46] N. Nagy, H.F. Kuipers, A.R. Frymoyer, H.D. Ishak, J.B. Bollyky, T.N. Wight, P. L. Bollyky, 4-Methylumbelliferone treatment and hyaluronan inhibition as a therapeutic strategy in inflammation, autoimmunity, and cancer, Front. Immunol. 6 (2015) 123, https://doi.org/10.3389/fimmu.2015.00123.
[47] T. Nakamura, M. Funahashi, K. Takagaki, H. Munakata, K. Tanaka, Y. Saito, M. Endo, Effect of 4-methylumbelliferone on cell-free synthesis of hyaluronic acid, Biochem. Mol. Biol. Int. 43 (1997) 263–268, https://doi.org/10.1080/15216549700204041.
[48] N. Nagy, et al., The pharmacokinetics and pharmacodynamics of 4-methylumbelliferone and its glucuronide metabolite in mice, in: A. Passi (Ed.), *Hyaluronan*, Biology of Extracellular Matrix, vol. 14, Springer, Cham, 2023, https://doi.org/10.1007/978-3-031-30300-5_8.
[49] J.H. Egedal, G. Xie, T.A. Packard, A. Laustsen, J. Neidleman, K. Georgiou, S. K. Pillai, W.C. Greene, M.R. Jakobsen, N.R. Roan, Hyaluronic acid is a negative regulator of mucosal fibroblast-mediated enhancement of HIV infection, Mucosal Immunol. 14 (2021) 1203–1213, https://doi.org/10.1038/s41385-021-00409-3.
[50] ClinicalTrials.gov, Evaluation of 4-methylumbelliferone for treatment of chronic hepatitis B (HBV) and chronic hepatitis C (HCV), Available from: https://clinicaltrials.gov/ct2/show/NCT00225537, 2006. (Accessed 22 July 2025).
[51] X. Li, H. Zeng, P. Wang, L. Lin, L. Liu, P. Zhen, Y. Fu, P. Lu, H. Zhu, Reactivation of latent HIV-1 in latently infected cells by coumarin compounds: hymecromone and scoparone, Curr. HIV Res. 14 (2016) 484–490, https://doi.org/10.2174/1570162x14666161003152458.
[52] D. O'Hagan, R.J. Young, Future challenges and opportunities with fluorine in drugs? Med. Chem. Res. 32 (2023) 1231–1234, https://doi.org/10.1007/s00044-023-03094-y.
[53] S. Kandil, J.M. Wymant, B.M. Kariuki, A.T. Jones, C. McGuigan, A.D. Westwell, Novel cis-selective and non-epimerisable C3 hydroxy azapodophyllotoxins targeting microtubules in cancer cells, Eur. J. Med. Chem. 110 (2016) 311–325, https://doi.org/10.1016/j.ejmech.2015.12.037.
[54] D.A. Dart, S. Kandil, S. Tommasini-Ghelfi, G. Serrano de Almeida, C.L. Bevan, W. Jiang, A.D. Westwell, Novel trifluoromethylated enobosarm analogues with potent antiandrogenic activity in vitro and tissue selectivity in vivo, Mol. Cancer Therapeut. 17 (2018) 1846–1858, https://doi.org/10.1158/1535-7163.MCT-18-0037.
[55] S.B. Kandil, C. McGuigan, A.D. Westwell, Synthesis and biological evaluation of bicalutamide analogues for the potential treatment of prostate cancer, Molecules 26 (2020) 56, https://doi.org/10.3390/molecules26010056.
[56] S.B. Kandil, B.M. Kariuki, C. McGuigan, A.D. Westwell, Synthesis, biological evaluation and X-ray analysis of bicalutamide sulfoxide analogues for the potential treatment of prostate cancer, Bioorg. Med. Chem. Lett. 36 (2021) 127817, https://doi.org/10.1016/j.bmcl.2021.127817.
[57] W. Hakamata, S. Tamura, T. Hirano, T. Nishio, Multicolor imaging of endoplasmic reticulum-located esterase as a prodrug activation enzyme, ACS Med. Chem. Lett. 5 (2014) 321–325.
[58] A. Beč, L. Racané, L. Žonja, L. Persoons, D. Daelemans, K. Starčević, R. Vianello, M. Hranjec, Biological evaluation of novel amidino substituted coumarin-benzazole hybrids as promising therapeutic agents, RSC Med. Chem. 14 (2023) 957–968, https://doi.org/10.1039/d3md00055a.
[59] I. Kostova, Coumarins as inhibitors of HIV reverse transcriptase, Curr. HIV Res. 4 (2006) 347–363.
[60] P. Wadhwa, P. Jain, S. Rudrawar, H.R. Jadhav, Quinoline, coumarin and other heterocyclic analogs based HIV-1 integrase inhibitors, Curr. Drug Discov. Technol. 15 (2018) 2–19.
[61] Z.Q. Liu, Is it still worth renewing nucleoside anticancer drugs nowadays? Eur. J. Med. Chem. 264 (2024) 115987 https://doi.org/10.1016/j.ejmech.2023.115987.

[62] P.S. Pennings, HIV drug resistance: problems and perspectives, Infect. Dis. Rep. 6 (2013) 5.
[63] A. Mullard, FDA approves twice-yearly capsid inhibitor for HIV prevention, Nat. Rev. Drug Discov. 24 (2025) 577, https://doi.org/10.1038/d41573-025-00117-8.
[64] H. Zahreddine, K.L. Borden, Mechanisms and insights into drug resistance in cancer, Front. Pharmacol. 4 (2013) 28.
[65] M. Slusarczyk, M.H. Lopez, J. Balzarini, M. Mason, W.G. Jiang, S. Blagden, E. Thompson, E. Ghazaly, C. McGuigan, Application of ProTide technology to gemcitabine: a successful approach to overcome the key cancer resistance mechanisms leads to a new agent (NUC-1031) in clinical development, J. Med. Chem. 57 (2014) 1531–1542, https://doi.org/10.1021/jm401853a.
[66] F.M. Uckun, S. Pendergrass, T.K. Venkatachalam, S. Qazi, D. Richman, Stampidine is a potent inhibitor of zidovudine- and nucleoside analog reverse transcriptase inhibitor-resistant primary clinical human immunodeficiency virus type 1 isolates with thymidine analog mutations, Antimicrob. Agents Chemother. 46 (2002) 3613–3616.
[67] P. Ryszkiewicz, B. Malinowska, E. Schlicker, Polypharmacology: promises and new drugs in 2022, Pharmacol. Rep. 75 (2023) 755–770, https://doi.org/10.1007/s43440-023-00501-4.
[68] A. Kabir, A. Muth, Polypharmacology: the science of multi-targeting molecules, Pharmacol. Res. 176 (2022) 106055, https://doi.org/10.1016/j.phrs.2021.106055.
[69] P. de Sena Murteira Pinheiro, L.S. Franco, T.L. Montagnoli, C.A.M. Fraga, Molecular hybridization: a powerful tool for multitarget drug discovery, Expet Opin. Drug Discov. 19 (2024) 451–470, https://doi.org/10.1080/17460441.2024.2322990.
[70] U. Pradere, E.C. Garnier-Amblard, S.J. Coats, F. Amblard, R.F. Schinazi, Synthesis of nucleoside phosphate and phosphonate prodrugs, Chem. Rev. 114 (2014) 9154–9218, https://doi.org/10.1021/cr5002035.
[71] a) National Poisons Information Service (NPIS), Phenol, TOXBASE® (2014);
b) M.D. Doherty, G.M. Cohen, M.T. Smith, Mechanisms of toxic injury to isolated hepatocytes by 1-naphthol, Biochem. Pharmacol. 33 (4) (1984) 543–549, https://doi.org/10.1016/0006-2952(84)90305-8;
c) J.W. owns, B.K. Wills, Phenol Toxicity [Updated 2023 Mar 13], in: StatPearls [Internet], StatPearls Publishing, Treasure Island (FL), 2025 Jan. Available from: https://www.gov.uk/government/publicayions/phenol-properties-incident-management-and-toxicology/phenol-toxicological-overview.
[72] J.J. Knox, M.G. McNamara, I.S. Bazin, D.Y. Oh, O. Zubkov, V. Breder, L.Y. Bai, A. Christie, L. Goyal, D.P. Cosgrove, C. Springfeld, K.M. Sjoquist, J.O. Park, H. Verdaguer, C. Braconi, P.J. Ross, A. De Gramont, R.T. Shroff, J.R. Zalcberg, D. H. Palmer, J.R. Smith, E. Oelmann, T. Bruce, J.W. Valle, A phase III randomized study of first-line NUC-1031/cisplatin vs. gemcitabine/cisplatin in advanced biliary tract cancer, J. Hepatol. 83 (2) (2025) 358–366, https://doi.org/10.1016/j.jhep.2025.01.040.
[73] S. Sandhu, Y. Bansal, O. Silakari, G. Bansal, Coumarin hybrids as novel therapeutic agents, Bioorg. Med. Chem. 22 (2014) 3806–3814, https://doi.org/10.1016/j.bmc.2014.05.032.
[74] S. Emami, S. Dadashpour, Current developments of coumarin-based anti-cancer agents in medicinal chemistry, Eur. J. Med. Chem. 102 (2015) 611–630, https://doi.org/10.1016/j.ejmech.2015.08.033.
[75] H. Schill, S. Nizamov, F. Bottanelli, J. Bierwagen, V.N. Belov, S.W. Hell, 4-Trifluoromethyl-substituted coumarins with large Stokes shifts: synthesis, bioconjugates, and their use in super-resolution fluorescence microscopy, Chemistry 19 (2013) 16556–16565, https://doi.org/10.1002/chem.201302037.
[76] A.R. Kore, B. Yang, B. Srinivasan, Efficient synthesis of terminal 4-methylumbelliferyl labeled 5-fluoro-2′-deoxyuridine-5′-O-tetraphosphate (Um-PPPP-FdU): a potential probe for homogenous fluorescent assay, Tetrahedron Lett. 55 (2014) 482, https://doi.org/10.1016/j.tetlet.2014.07.014.
[77] C. McGuigan, H.W. Tsang, D. Cahard, K. Turner, S. Velazquez, A. Salgado, L. Bidois, L. Naesens, E. De Clercq, J. Balzarini, Phosphoramidate derivatives of d4T as inhibitors of HIV: the effect of amino acid variation, Antivir. Res. 35 (1997) 195–204.
[78] C. McGuigan, K.G. Devine, T.J. O'Connor, D. Kinchington, Synthesis and anti-HIV activity of some haloalkyl phosphoramidate derivatives of 3'-azido-3'-deoxythymidine (AZT): potent activity of the trichloroethyl methoxyalaninyl compound, Antivir. Res. 15 (1991) 255–263.
[79] B.S. Ross, P.G. Reddy, H.R. Zhang, S. Rachakonda, M.J. Sofia, Synthesis of diastereomerically pure nucleotide phosphoramidates, J. Org. Chem. 76 (2011) 8311–8319, https://doi.org/10.1021/jo201492m.
[80] B. Simmons, Z. Liu, A. Klapars, A. Bellomo, S.M. Silverman, Mechanism-based solution to the ProTide synthesis problem: selective access to sofosbuvir, acelarin, and INX-08189, Org. Lett. 19 (2017) 2218–2221, https://doi.org/10.1021/acs.orglett.7b00469.
[81] C. Pannecouque, D. Daelemans, E. De Clercq, Tetrazolium-based colorimetric assay for the detection of HIV replication inhibitors: revisited 20 years later, Nat. Protoc. 3 (2008) 427–434.
[82] D. Kang, D. Feng, T. Ginex, J. Zou, F. Wei, T. Zhao, B. Huang, Y. Sun, S. Desta, E. De Clercq, C. Pannecouque, P. Zhan, X. Liu, Exploring the hydrophobic channel of NNIBP leads to the discovery of novel piperidine-substituted thiophene[3,2-d] pyrimidine derivatives as potent HIV-1 NNRTIs, Acta Pharm. Sin. B 10 (2020) 878–894.
[83] W. Gu, S. Martinez, H. Nguyen, H. Xu, P. Herdewijn, S. De Jonghe, K. Das, Tenofovir-amino acid conjugates act as polymerase substrates – implications for avoiding cellular phosphorylation in the discovery of nucleotide analogues, J. Med. Chem. 64 (2021) 782–796, https://doi.org/10.1021/acs.jmedchem.0c01747.
[84] K.M. Glockzin, T. Narindoshvili, F.M. Raushel, Regiochemical analysis of the ProTide activation mechanism, Biochemistry 63 (2024) 1774–1782, https://doi.org/10.1021/acs.biochem.4c00176.
[85] A.Q. Siddiqui, C. McGuigan, C. Ballatore, F. Zuccotto, I.H. Gilbert, E. De Clercq, J. Balzarini, Design and synthesis of lipophilic phosphoramidate d4T-MP prodrugs expressing high potency against HIV in cell culture: structural determinants for in vitro activity and QSAR, J. Med. Chem. 42 (1999) 4122–4128, https://doi.org/10.1021/jm9807104.
[86] E. Procházková, H. Hřebabecký, M. Dejmek, M. Šála, M. Šmídková, E. Tloušťová, E. Zborníková, L. Eyer, D. Růžek, R. Nencka, Could 5'-N and S ProTide analogues work as prodrugs of antiviral agents? Bioorg. Med. Chem. Lett. 30 (2020) 126897 https://doi.org/10.1016/j.bmcl.2019.126897.
[87] S. Kar, J. Leszczynski, Open access in silico tools to predict the ADMET profiling of drug candidates, Expet Opin. Drug Discov. 15 (2020) 1473–1487, https://doi.org/10.1080/17460441.2020.1798926.
[88] A. Daina, O. Michielin, V. Zoete, SwissADME: a free web tool to evaluate pharmacokinetics, drug-likeness and medicinal chemistry friendliness of small molecules, Sci. Rep. 7 (2017) 42717, https://doi.org/10.1038/srep42717.